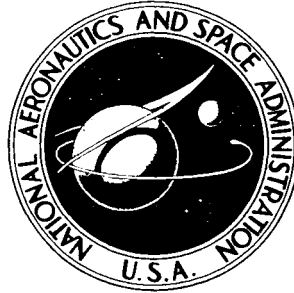


**NASA TECHNICAL
MEMORANDUM**



NASA TM X-1176

NASA TM X-1176

**EFFECTS OF TIP-FIN GEOMETRY ON
STABILITY CHARACTERISTICS OF A
MANNED LIFTING ENTRY VEHICLE
FROM MACH 1.50 TO 2.86**

by James F. Campbell
Langley Research Center
Langley Station, Hampton, Va.

EFFECTS OF TIP-FIN GEOMETRY ON STABILITY CHARACTERISTICS
OF A MANNED LIFTING ENTRY VEHICLE FROM MACH 1.50 TO 2.86

By James F. Campbell

Langley Research Center
Langley Station, Hampton, Va.

EFFECTS OF TIP-FIN GEOMETRY ON STABILITY CHARACTERISTICS
OF A MANNED LIFTING ENTRY VEHICLE FROM MACH 1.50 TO 2.86*

By James F. Campbell
Langley Research Center

SUMMARY

An investigation was conducted in the Langley Unitary Plan wind tunnel at Mach numbers from 1.50 to 2.86 to determine the effects of variations in tip-fin geometry on the stability characteristics of a manned lifting entry vehicle, designated HL-10. The results of this investigation indicate that increasing the toe-in angle of the tip-fin upper and lower panels combined or just the tip-fin upper panel generally resulted in increases in the directional stability parameter and the effective dihedral throughout the test angle-of-attack and Mach number ranges; the most important tip-fin geometric change, however, appeared to be that of the lower panel. Increasing the tip-fin upper-panel planform area produced substantial increases in the directional stability parameter and in the effective dihedral parameter throughout the test angle-of-attack and Mach number ranges. Varying tip-fin roll-out and toe-in angles and lateral planform area had only minor effects on the longitudinal characteristics throughout the test angle-of-attack and Mach number ranges. It was also shown that, although placement of the directional-control flap on the outer surface of the tip-fin upper panel proved to be an effective means of producing yawing-moment control with no corresponding effects on longitudinal stability, there were significant amounts of adverse rolling moment throughout the test angle-of-attack and Mach number ranges.

INTRODUCTION

Configurations having moderate lift-drag ratios (on the order of 1.0 at hypersonic speeds) are of considerable interest for future entry vehicles. However, because these entry configurations are expected to operate over a wide range of angles of attack and Mach numbers during the entry mode, the attainment of adequate stability may be a critical factor. One of these configurations, designated HL-10, is undergoing concentrated study at the NASA Langley Research Center (refs. 1 to 7). These investigations have indicated that the negative cambered HL-10 lifting entry configuration must depend largely upon tip-fin surfaces for directional stability at the higher operational angles of attack in the supersonic and hypersonic speed regimes. Results (ref. 6) show that

*Title, Unclassified.

directional instability occurs in a limited angle-of-attack range for this basic version of the HL-10 entry vehicle at low supersonic speeds.

The present investigation was performed in order to determine the effects of variations in tip-fin geometry on the stability characteristics, and in particular, the directional stability of a model of the HL-10 entry vehicle at Mach numbers from 1.50 to 2.86. The tests were performed in the Langley Unitary Plan wind tunnel at angles of attack from about 0° to 38° and at angles of sideslip from about -4° to 8° . The Reynolds number per foot (per 30.5 cm) for these tests was 1.6×10^6 .

SYMBOLS

The lateral force and moment data are referred to the body-axis system and the longitudinal force and moment data are referred to the stability-axis system. The reference center of moments was located at 53 percent of the body length aft of the nose and at 1.25 percent of the body length below the body reference line.

The units for the physical quantities used in this paper are presented both in U.S. Customary Units and in the International System of Units (SI). Factors relating the two systems are given in reference 8.

b	body reference span, 10.310 in. (26.2 cm)
l	body reference length, 16.000 in. (40.6 cm)
L/D	lift-drag ratio, $\frac{C_L}{C_D}$
C_L	lift coefficient, $\frac{\text{Lift}}{qS}$
C_D	drag coefficient, $\frac{\text{Drag}}{qS}$
C_m	pitching-moment coefficient, $\frac{\text{Pitching moment}}{qSl}$
C_l	rolling-moment coefficient, $\frac{\text{Rolling moment}}{qSb}$
C_{l_β}	effective-dihedral parameter, $\frac{\Delta C_l}{\Delta \beta}$, per deg
C_n	yawing-moment coefficient, $\frac{\text{Yawing moment}}{qSb}$

$C_{n\beta}$	directional-stability parameter, $\frac{\Delta C_n}{\Delta \beta}$, per deg
C_Y	side-force coefficient, $\frac{\text{Side force}}{qS}$
$C_{Y\beta}$	side-force parameter, $\frac{\Delta C_Y}{\Delta \beta}$, per deg
M	free-stream Mach number
q	free-stream dynamic pressure
r	radius, in. (cm)
S	reference planform area, 0.634 sq ft. (0.0589 m ²)
S*	planform area of tip-fin panel, sq in. (cm ²)
X,Y,Z	body-axis system
x,y,z	coordinates defining model contours
α	angle of attack of model referred to body-reference line, deg
β	angle of sideslip of model referred to plane of symmetry, deg
θ	angle of aft lower surface of model in X-Z plane, 15°
ϵ	true toe-in angle of the tip fins ($\phi = 0$) in X-Y plane, deg
ϕ	roll-out angle of outside surface of tip fin; hinge line for roll-out of lower panel is in plane of lower surface of body, deg

Subscripts:

1	lower panel
2	upper panel

APPARATUS AND TESTS

Wind Tunnel

Tests were conducted in the low Mach number test section of the Langley Unitary Plan wind tunnel, which is a variable-pressure continuous-flow tunnel. The test section is approximately 4 feet (1.22 m) square and 7 feet (2.13 m) long. The nozzle leading to the test section is of the asymmetric, sliding-block type which permits a continuous variation in Mach number from about 1.5 to 2.9.

Model

Details of the 74° swept-leading-edge model are presented in figure 1 and ordinates defining the profile and cross-section shape of the model, in table I. The various tip-fin arrangements investigated are shown in figure 2, which illustrates the planform details when viewed perpendicular to each panel outer chord plane along with upper-panel hinge-line locations. Tip-fin geometric characteristics projected on either the plane of symmetry or the longitudinal plane for the test arrangements may be obtained from the dimensions of figure 2 by considerations of the angular orientation (table II) of each panel in the horizontal and vertical planes. A summary of the geometric variables and tip-fin details is presented in table II. Photographs of two configurations are shown in figure 3. A wedge simulating a directional-control flap having a deflection of 20° was provided on the outer surface of the left tip-fin (P_2) upper panel (fig. 2).

Test Conditions

The test conditions for the investigation were as follows:

Mach number	Stagnation temperature		Stagnation pressure	
	$^\circ\text{F}$	$^\circ\text{K}$	psia	kN/m^2
1.50	150	339	6.18	42.6
1.80	150	339	6.78	46.8
2.16	150	339	7.92	54.6
2.86	150	339	11.39	78.5

The Reynolds number per foot (per 30.5 cm) was constant at 1.6×10^6 for all test conditions. The stagnation dewpoint was maintained at -30°F (239°K) in order to avoid condensation effects in the test section. The angle-of-attack range of the tests extended from about 0° to 38° and the angle-of-sideslip range from about -4° to 8° .

Measurements

Aerodynamic forces and moments were measured by six-component electrical strain-gage balance housed within the model. The balance, in turn, was rigidly fastened to a sting support and thence to the tunnel support system.

Accuracy

The accuracy of the individual measured quantities, based on calibration and repeatability of data, is estimated to be within the following limits:

C_D	± 0.001
C_L	± 0.004
C_l	± 0.0002
C_m	± 0.0004
C_n	± 0.0002
C_Y	± 0.001
α , deg	± 0.10
β , deg	± 0.10
M	± 0.015

Corrections

Angles of attack were corrected for tunnel-flow angularity, and angles of attack and sideslip were corrected for deflection of the balance and sting support due to aerodynamic loads. The drag data presented are the values measured by the strain-gage balance with no adjustment made to relate drag levels to a condition corresponding to free-stream static-pressure conditions at the model base.

PRESENTATION OF RESULTS

Results of the investigation of effects of tip-fin geometry on stability characteristics of a manned lifting entry vehicle are presented in the following figures:

Schlieren photographs	4
Basic lateral characteristics -	
Effect of P_1 tip-fin toe-in angle	5
Effect of upper-panel toe-in angle	6
Effect of upper-panel planform area	7
Effect of upper-panel roll-out angle	8
Lateral parameters -	
Effect of P_1 tip-fin toe-in angle	9
Effect of upper-panel toe-in angle	10
Effect of upper-panel planform area	11
Effect of upper-panel roll-out angle	12
Effect of left P_2 tip-fin upper-panel control-surface deflection	13
Longitudinal characteristics -	
Effect of P_1 tip-fin toe-in angle	14
Effect of upper-panel toe-in angle	15
Effect of upper-panel planform area	16
Effect of upper-panel roll-out angle	17
Effect of P_2 left tip-fin upper-panel control-surface deflection	18

DISCUSSION

Lateral Characteristics

The basic aerodynamic characteristics in sideslip at Mach numbers 1.50 and 2.86 are presented in order to indicate the effects of tip-fin geometry on the linearity of the lateral coefficients at an angle of attack in the vicinity of minimum $C_{n\beta}$ (figs. 5 to 8). Since the sideslip parameters presented herein (figs. 9 to 12) were obtained from incremental differences between results of tests made through the angle-of-attack range at fixed angles of sideslip of about 0° and 5° , the linearity can affect the quantitative results. The basic lateral coefficient results are relatively linear up to a sideslip angle at 5° at $M = 2.86$; however, some nonlinearities are evident, particularly in yawing moment, at $M = 1.50$. It is believed that while the values of $C_{n\beta}$ at $M = 1.50$ (figs. 9 to 12) differ from the slopes obtained at $\beta = 0^\circ$ (figs. 5 to 8), the trends of the comparative curves are accurately defined.

Increasing the toe-in angle of the tip-fin upper and lower panels combined (fig. 9) or just the tip-fin upper panel (fig. 10) generally results in a positive increment in the directional stability parameter throughout the test angle-of-attack and Mach number ranges. Comparison of the directional-stability data of the two figures indicates that the most important geometric change affecting the directional stability level is that of the lower panel. Increases in the directional stability parameter are also realized by increasing the tip-fin upper-panel planform area (fig. 11). It should be noted that, in the vicinity of the angle of attack at which minimum directional stability occurs for $M = 1.50$, there appears to be a reversal in the general trends of $C_{n\beta}$ noted previously in figures 9 to 11. The reason for these unexpected reversals is not presently known.

It is seen by comparison of the P_2 and S tip fins (fig. 12) that increasing the tip-fin upper-panel roll-out angle has a favorable effect on the directional stability parameter and causes an increase in $C_{n\beta}$ throughout the test angle-of-attack and Mach number ranges. The increased roll-out and toe-in angles associated with the T tip-fin configuration result in a substantial increase in the directional stability level over those corresponding to the P_2 and S tip fins at angles of attack in the vicinity of minimum $C_{n\beta}$ at all test Mach numbers. The characteristic of the T tip fins to provide the highest level of directional stability at angles of attack in the vicinity of minimum $C_{n\beta}$ holds true when these data are compared with those of the other tip fins tested, particularly at a Mach number of 1.50.

The tip-fin geometric changes that improved the directional stability characteristics of these configurations also caused an increase in effective dihedral ($-C_{l\beta}$) throughout the test angle-of-attack and Mach number ranges. These results are caused by the tip-fin orientation aft and above the model center of gravity. The T tip fins provide the largest amount of effective

dihedral at angles of attack in the vicinity of minimum $C_{n\beta}$, particularly at a Mach number of 1.50.

Placement of the directional flap on the outer surface of the P_2 left tip-fin upper-panel is an effective means of providing yawing moment for directional control at all test angles of attack and Mach numbers (fig. 13) although significant amounts of adverse rolling moment were also induced. No cross effects of this rudder flap on the longitudinal characteristics were noted (fig. 18).

Longitudinal Characteristics

The effects of increased toe-in angle of the P_1 tip fins are seen in figure 14 as an increase in stability, an increase in C_D , and a corresponding decrease in L/D at all test Mach numbers. Although these effects might be expected considering the orientation of the lower and upper panel surfaces of the tip fin in a combined roll-out and toe-in configuration, the variation of the upper-panel toe-in angle alone (fig. 15) has no effect on the longitudinal characteristics. Increasing upper-panel planform area (fig. 16) primarily results in increases in α_{trim} . This effect of planform area essentially disappears at the highest test Mach number. The results of increased upper-panel roll-out angle seen by comparing P_2 and S tip fins (fig. 17) show a slight decrease in α_{trim} with little or no effect on C_D , L/D , or C_L throughout the test Mach number range. The increase in roll-out and toe-in angles associated with the T tip fins over those of the P_2 and S tip fins results in lower values of α_{trim} and a substantial increase in stability. In addition, higher values of both C_L and C_D were obtained but the maximum values of L/D were less.

CONCLUSIONS

Tests to determine the effects of tip-fin geometry on the stability characteristics of a basic version of a manned lifting entry vehicle, designated HL-10, at Mach numbers from 1.50 to 2.86 indicated the following conclusions:

1. Increasing the toe-in angle of the tip-fin upper and lower panels combined or just the tip-fin upper panel generally resulted in increases in the directional stability parameter and the effective dihedral throughout the test angle-of-attack and Mach number ranges; the most important tip-fin geometric change, however, appeared to be that of the lower panel.
2. Increasing the tip-fin upper-panel planform area produced substantial increases in the directional stability parameter and in the effective dihedral parameter throughout the test angle-of-attack and Mach number ranges.
3. Varying tip-fin roll-out and toe-in angles and lateral planform area had only minor effects on the longitudinal characteristics throughout the test angle-of-attack and Mach number ranges.

4. Although placement of the directional-control flap on the outer surface of the tip-fin upper panel proved to be an effective means of producing yawing-moment control with no corresponding effects on longitudinal stability, there were significant amounts of adverse rolling moment throughout the test angle-of-attack and Mach number ranges.

Langley Research Center,
National Aeronautics and Space Administration,
Langley Station, Hampton, Va., July 22, 1965.

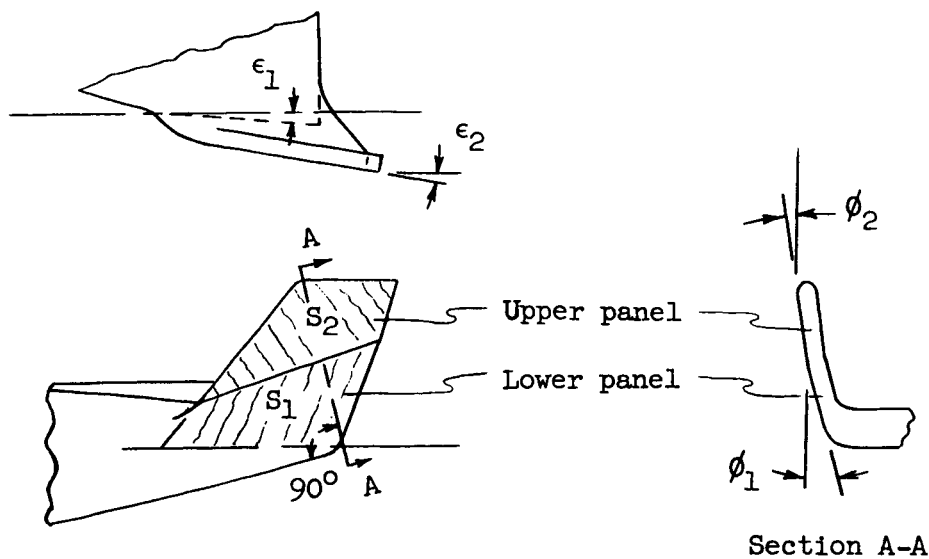
REFERENCES

1. Ware, George M.: Aerodynamic Characteristics of Models of Two Thick 74° Delta Manned Lifting Entry Vehicles at Low-Subsonic Speeds. NASA TM X-914, 1964.
2. Rainey, Robert W.; and Ladson, Charles L.: Preliminary Aerodynamic Characteristics of a Manned Lifting Entry Vehicle at a Mach Number of 6.8. NASA TM X-844, 1963.
3. Ladson, Charles L.: Aerodynamic Characteristics of a Manned Lifting Entry Vehicle at a Mach Number of 6.8. NASA TM X-915, 1964.
4. Silvers, H. Norman; and Campbell, James F.: Stability Characteristics of a Manned Lifting Entry Vehicle With Various Fins at Mach Numbers From 1.50 to 2.86. NASA TM X-1161, 1965.
5. McShera, John T., Jr.; and Campbell, James F.: Aerodynamic Characteristics From Mach 1.50 to 2.86 of a Lifting Entry Vehicle Alone, With Adapter Sections, and With a Saturn Launch Vehicle. NASA TM X-1125, 1965.
6. Campbell, James F.; and McShera, John T., Jr.: Stability and Control Characteristics From Mach Number 1.50 to 2.86 of a Model of a Manned Lifting Entry Vehicle. NASA TM X-1117, 1965.
7. McShera, John T., Jr.; and Campbell, James F.: Stability and Control Characteristics of a Lifting Entry Vehicle at Mach Numbers From 2.29 to 4.63. NASA TM X-1019, 1964.
8. Mechtly, E. A.: The International System of Units - Physical Quantities and Conversion Factors. NASA SP-7012, 1964.

TABLE I.- ORDINATES DEFINING CROSS-SECTIONAL SHAPE OF HL-10 WITHOUT TIP FINS

z/l	y/l	z/l	y/l	z/l	y/l	z/l	y/l	z/l	y/l	z/l	y/l	z/l	y/l	z/l	y/l
$x/l = 0.042$		$x/l = 0.208$		$x/l = 0.292$		$x/l = 0.417$		$x/l = 0.500$		$x/l = 0.583$		$x/l = 0.667$		$x/l = 0.792$	
0.0541	0	0.0792	0	-0.0167	0.1119	0.0814	0	0.0782	0	0.0741	0	0.0553	0.1541	0.0578	0
.0532	.0083	.0787	.0083	-.0250	.1137	.0813	.0083	.0782	.0167	.0741	.0104	.0522	.1624	.0577	.0937
.0503	.0167	.0772	.0167	-.0333	.1156	.0811	.0167	.0780	.0250	.0740	.0271	.0483	.1708	.0576	.1104
.0441	.0250	.0747	.0250	-.0417	.1170	.0805	.0250	.0776	.0333	.0735	.0437	.0439	.1791	.0573	.1270
.0375	.0306	.0712	.0333	-.0500	.1182	.0797	.0333	.0770	.0417	.0726	.0604	.0385	.1874	.0569	.1437
.0333	.0338	.0664	.0416	-.0583	.1192	.0786	.0417	.0762	.0500	.0710	.0771	.0317	.1958	.0561	.1604
.0250	.0390	.0592	.0500	-.0667	.1198	.0772	.0500	.0751	.0583	.0671	.0937	.0250	.2015	.0549	.1770
.0167	.0431	.0517	.0583	-.0750	.1202	.0755	.0583	.0738	.0667	.0668	.1020	.0167	.2080	.0532	.1937
.0083	.0459	.0417	.0656	-.1268	0	.0733	.0667	.0723	.0750	.0651	.1104	.0083	.2128	.0506	.2103
0	.0476	.0333	.0713			.0706	.0750	.0705	.0833	.0626	.1187	0	.2167	.0486	.2187
-.0536	0	.0250	.0760	$x/l = 0.333$.0674	.0833	.0682	.0917	.0596	.1270	-.0083	.2197	.0460	.2270
		.0167	.0800			.0633	.0917	.0655	.1000	.0563	.1354	-.0167	.2218	.0425	.2353
$x/l = 0.083$.0083	.0833	0.0820	0	.0582	.1000	.0620	.1083	.0521	.1437	-.0250	.2237	.0375	.2437
		0	.0860	.0818	.0083	.0517	.1083	.0579	.1167	.0471	.1520	-.0333	.2254	.0333	.2481
0.0681	0	-.0083	.0882	.0813	.0167	.0437	.1167	.0529	.1250	.0412	.1604	-.0417	.2264	.0250	.2551
.0668	.0083	-.0167	.0902	.0803	.0250	.0375	.1211	.0467	.1333	.0337	.1687	-.0986	0	.0167	.2588
.0637	.0167	-.0250	.0919	.0789	.0333	.0333	.1241	.0390	.1417	.0250	.1756			.0083	.2611
.0579	.0250	-.0333	.0933	.0771	.0417	.0250	.1296	.0333	.1458	.0167	.1813	$x/l = 0.708$		0	.2624
.0502	.0333	-.0417	.0946	.0747	.0500	.0167	.1339	.0250	.1521	.0083	.1860	0.0654	0	-.0083	.2631
.0417	.0392	-.0500	.0955	.0716	.0583	.0083	.1375	.0167	.1571	0	.1897	0.0654	.0417	-.0167	.2634
.0330	.0444	-.0583	.0962	.0677	.0667	0	.1406	.0083	.1612	-.0083	.1926	.0653	.0534	-.0673	0
.0250	.0487	-.1126	0	.0627	.0750	-.0083	.1431	0	.1643	-.0167	.1949	.0651	.0583	$x/l = 0.833$	
.0167	.0521			.0564	.0833	-.0167	.1453	-.0083	.1672	-.0250	.1970	.0650	.0750	0.0536	0
.0083	.0547	$x/l = 0.250$.0485	.0917	-.0250	.1472	-.0167	.1694	-.0333	.1988	.0643	.0916	.0534	.1666
0	.0568			.0417	.0968	-.0333	.1492	-.0250	.1715	-.0417	.2003	.0634	.1083	.0532	.1833
-.0083	.0585	0.0807	0	.0333	.1027	-.0417	.1508	-.0333	.1733	-.0500	.2017	.0617	.1250	.0521	.1999
-.0167	.0596	.0803	.0083	.0250	.1078	-.0500	.1523	-.0417	.1750	-.0583	.2028	.0596	.1416	.0510	.2166
-.0752	0	.0792	.0167	.0167	.1119	-.0583	.1536	-.0500	.1763	-.1156	0	.0582	.1499	.0482	.2332
$x/l = 0.125$.0773	.0250	.0083	.1152	-.0667	.1546	-.0583	.1775			.0563	.1583	.0455	.2582
		.0748	.0333	0	.1179	-.0750	.1554	-.0667	.1785	$x/l = 0.625$.0542	.1666	.0400	.2666
		.0712	.0417	-.0083	.1204	-.0833	.1559	-.0750	.1792	0.0716	0	.0517	.1749	.0333	.2707
0.0737	0	.0666	.0500	-.0167	.1227	-.1340	0	-.1285	0	.0716	.0104	.0487	.1833	.0250	.2736
.0729	.0083	.0606	.0583	-.0250	.1250					.0716	.0271	.0446	.1916	.0167	.2749
.0702	.0167	.0527	.0667	-.0333	.1267	$x/l = 0.458$		$x/l = 0.542$.0716	.0398	.0446	.1999	.0083	.2753
.0660	.0250	.0458	.0721	-.0417	.1282	0.0800	0	0.0759	0	.0713	.0437	.0340	.2083	0	.2753
.0594	.0330	.0417	.0754	-.0500	.1296	.0799	.0083	.0759	.0166	.0707	.0604	.0292	.2130	-.0563	0
.0505	.0417	.0333	.0811	-.0583	.1306	.0797	.0167	.0758	.0249	.0696	.0771	.0250	.2168	$x/l = 0.875$	
.0417	.0477	.0250	.0862	-.0667	.1317	.0794	.0250	.0756	.0332	.0678	.0937	.0167	.2235	0.0487	0
.0333	.0528	.0167	.0902	-.0750	.1321	.0788	.0333	.0752	.0415	.0655	.1104	.0083	.2283	-.0452	0
.0250	.0571	.0083	.0937	-.1312	0	.0780	.0417	.0747	.0498	.0637	.1187	0	.2317	$x/l = 0.917$	
.0167	.0604	0	.0965			.0768	.0500	.0740	.0581	.0616	.1270	-.0083	.2343	0.0440	0
.0083	.0632	-.0083	.0990	$x/l = 0.375$.0755	.0583	.0730	.0664	.0591	.1354	-.0167	.2363	-.0341	0
0	.0656	-.0167	.1011			.0739	.0667	.0718	.0747	.0558	.1437	-.0250	.2378	$x/l = 0.958$	
-.0083	.0675	-.0250	.1027	0.0821	0	.0720	.0750	.0705	.0830	.0521	.1520	-.0333	.2390	0.0392	0
-.0167	.0691	-.0333	.1044	.0820	.0083	.0694	.0833	.0688	.0913	.0478	.1604	-.0889	0	-.0227	0
-.0250	.0704	-.0417	.1057	.0816	.0167	.0664	.0917	.0666	.0996	.0429	.1687	$x/l = 0.750$		$x/l = 1.000$	
-.0333	.0714	-.0500	.1067	.0809	.0250	.0629	.1000	.0642	.1079	.0365	.1770	0.0617	0	0.0344	0
-.0904	0	-.0583	.1076	.0799	.0333	.0581	.1083	.0611	.1162	.0292	.1842	.0611	.0958	-.0125	0
		-.0667	.1083	.0783	.0417	.0526	.1167	.0575	.1245	.0250	.1878	.0611	.1058		
$x/l = 0.167$		-.1205	0	.0766	.0500	.0453	.1250	.0530	.1328	.0167	.1941	.0611	.1125		
				.0744	.0583	.0363	.1333	.0476	.1411	.0083	.1991	.0606	.1191		
0.0771	0	$x/l = 0.292$.0714	.0667	.0292	.1379	.0410	.1494	-.0083	.2057	.0596	.1291		
.0763	.0083			.0679	.0750	.0250	.1407	.0326	.1577	-.0167	.2080	.0581	.1458		
.0744	.0167	0.0817	0	.0633	.0833	.0200	.1454	.0249	.1629	-.0250	.2101	.0561	.1624		
.0712	.0250	.0814	.0083	.0576	.0917	.0167	.1491	.0166	.1685	-.0333	.2118	.0533	.1791		
.0664	.0333	.0807	.0167	.0503	.1000	.0083	.1521	.0083	.1729	-.0417	.2132	.0488	.1958		
.0597	.0417	.0794	.0250	.0415	.1083	0	.1549	0	.1764	-.0500	.2143	.0458	.2041		
.0512	.0500	.0774	.0333	.0333	.1136	-.0083	.1571	-.0083	.1790	-.1073	0	.0421	.2124		
.0417	.0565	.0750	.0417	.0250	.1187	-.0167	.1592	-.0166	.1815	$x/l = 0.667$.0372	.2207		
.0333	.0618	.0715	.0500	.0167	.1229	-.0250	.1611	-.0249	.1834	0.0687	0	.0333	.2256		
.0250	.0664	.0672	.0583	.0083	.1262	-.0333	.1627	-.0332	.1853	.0686	.0208	.0292	.2307		
.0167	.0701	.0617	.0667	0	.1292	-.0417	.1642	-.0415	.1869	.0686	.0375	.0250	.2347		
.0083	.0732	.0546	.0750	-.0083	.1315	-.0500	.1664	-.0498	.1882	.0684	.0541	.0167	.2409		
0	.0757	.0500	.0789	-.0167	.1337	-.0583	.1684	-.0581	.1893	.0678	.0708	0	.2447		
-.0083	.0778	.0417	.0858	-.0250	.1358	-.0667	.1694	-.0664	.1902	.0669	.0875	-.0083	.2470		
-.0167	.0796	.0333	.0918	-.0333	.1377	-.0750	.1712			.0655	.1041	-.0167	.2504		
-.0250	.0811	.0250	.0969	-.0417	.1394	-.0833	.1722			.0634	.1208	-.0250	.2511		
-.0333	.0823	.0167	.1010	-.0500	.1408	-.1322	0			.0601	.1374	-.0785	0		
-.0417	.0833	.0083	.1044	-.0583	.1420					.0580	.1458				
-.0500	.0840	0	.1072	-.0667	.1429										
-.1026	0	-.0083	.1098	-.0750	.1437										
				-.0833	.1442										
				-.1334	0										

TABLE II.- DEFINITION OF TIP-FIN GEOMETRIC PARAMETERS
 [Presented area is panel chord-plane area]



Designation	Lower panel				Upper panel			
	ϵ_1 , deg	ϕ_1 , deg	S_1^*		ϵ_2 , deg	ϕ_2 , deg	S_2^*	
			in ²	cm ²			in ²	cm ²
P ₁	5	15	5.0	32.25	0	0	5.0	32.25
P ₂	↓	↓	↓		5	↓	↓	
P ₃	↓	↓	↓		10	↓	↓	
Q	↓	↓	↓		5	↓	2.5	16.13
R	↓	↓	↓		↓	↓	7.5	48.38
S	↓	↓	↓		↓	15	5.0	32.25
T	16	30						

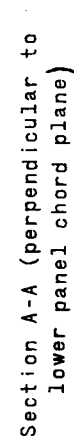
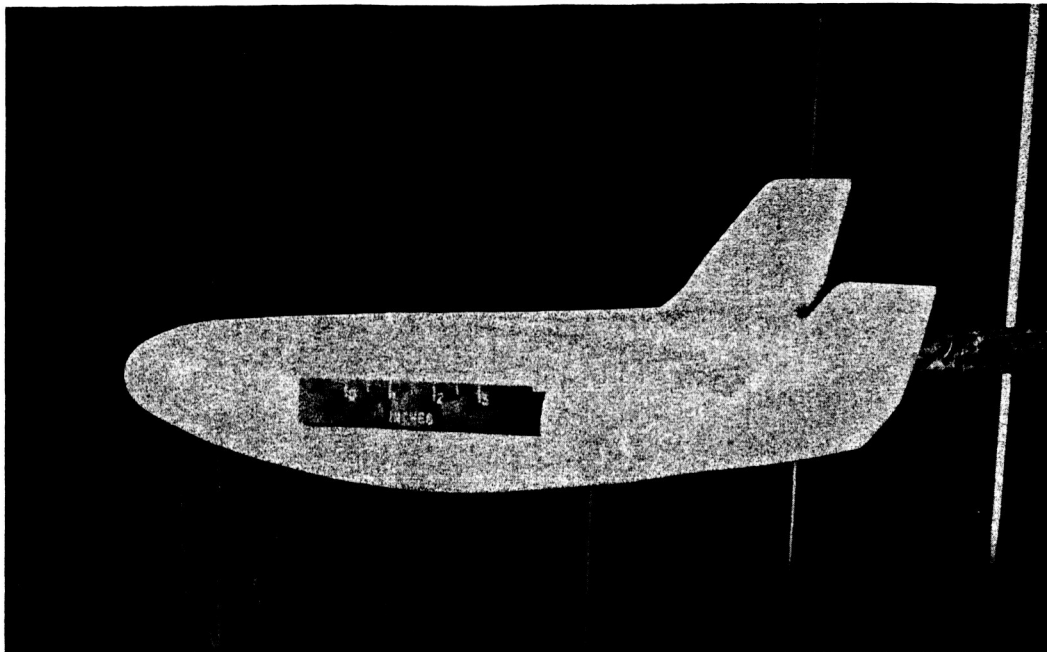


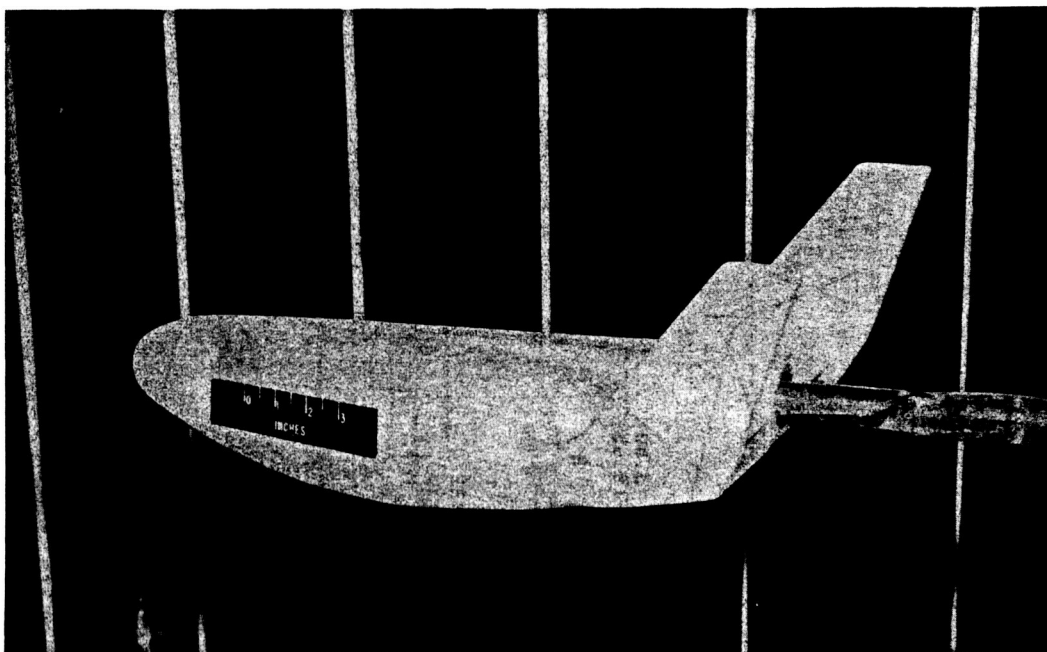
Figure 1.- Drawing of test model with P₃ tip fins. (All dimensions are in inches unless otherwise specified; parenthetical dimensions are in centimeters.)

Figure 2.- Tip-fin configurations viewed perpendicular to each panel chord plane. (All dimensions are in inches unless otherwise specified; parenthetical dimensions are in centimeters.)



P₃ tip fin

L-64-2484



R tip fin

L-64-2488

Figure 5.- Photographs of the test model mounted in the Langley Unitary Plan wind tunnel.



$\alpha = 0.30^\circ$



$\alpha = 19.23^\circ$



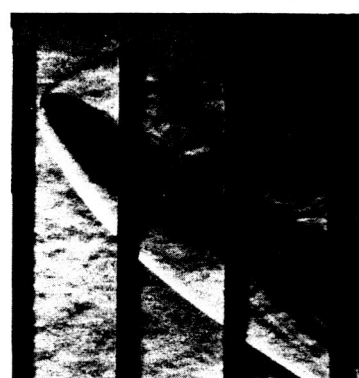
$\alpha = 37.97^\circ$



$\alpha = -0.10^\circ$



$\alpha = 16.35^\circ$

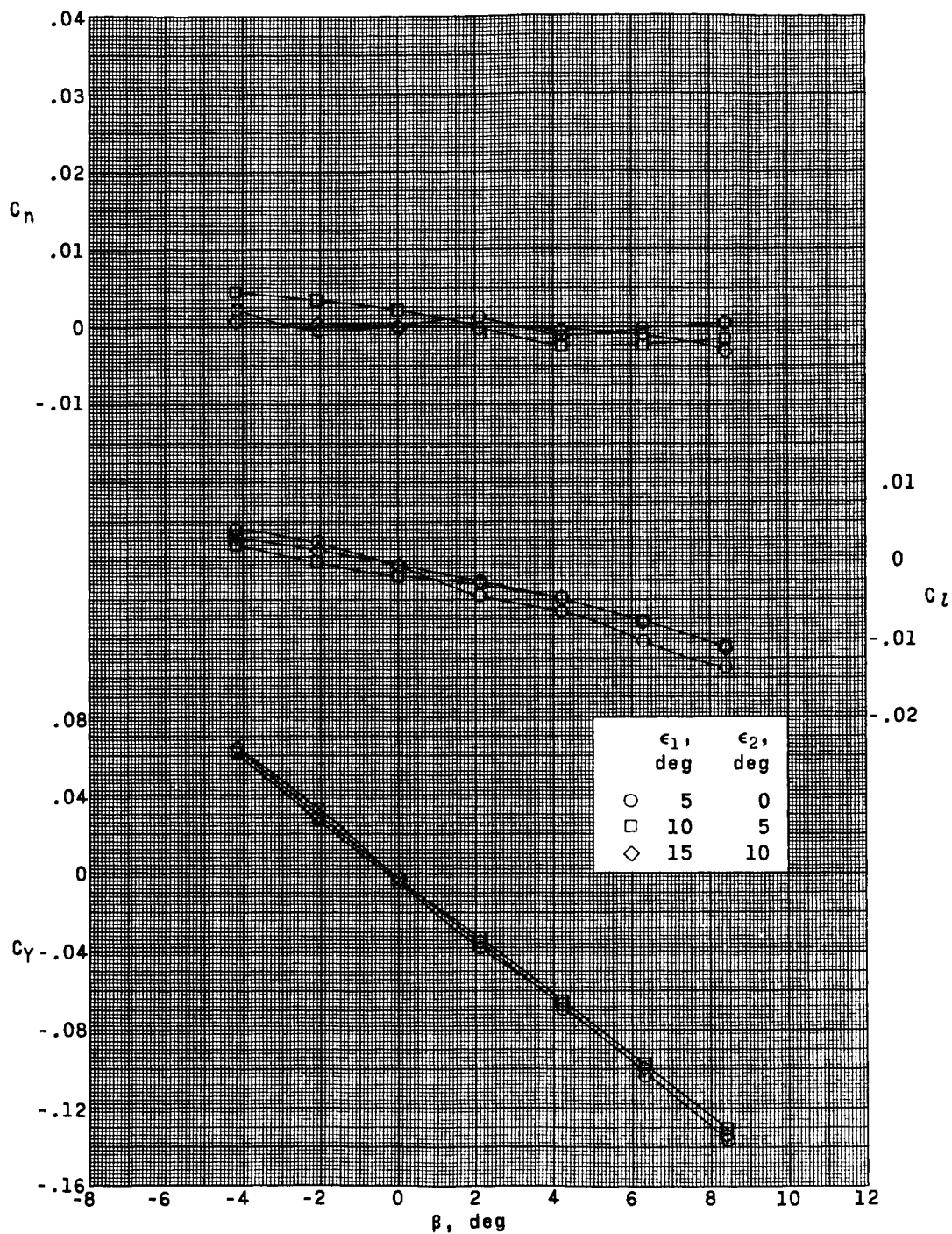


$\alpha = 36.86^\circ$

$M = 2.86$

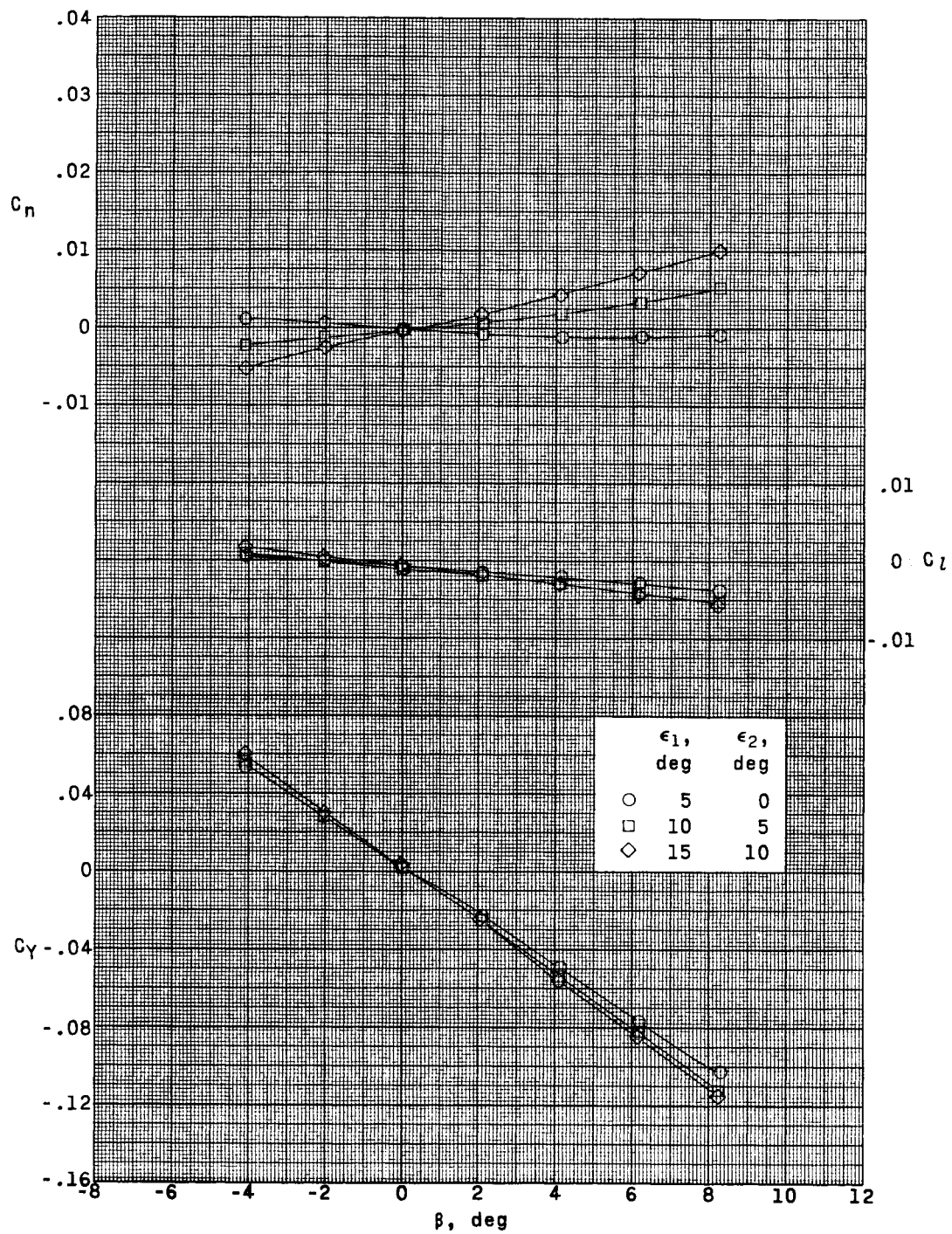
Figure 4.- Schlieren photographs of the test model with P_1 tip fin.

L-65-169



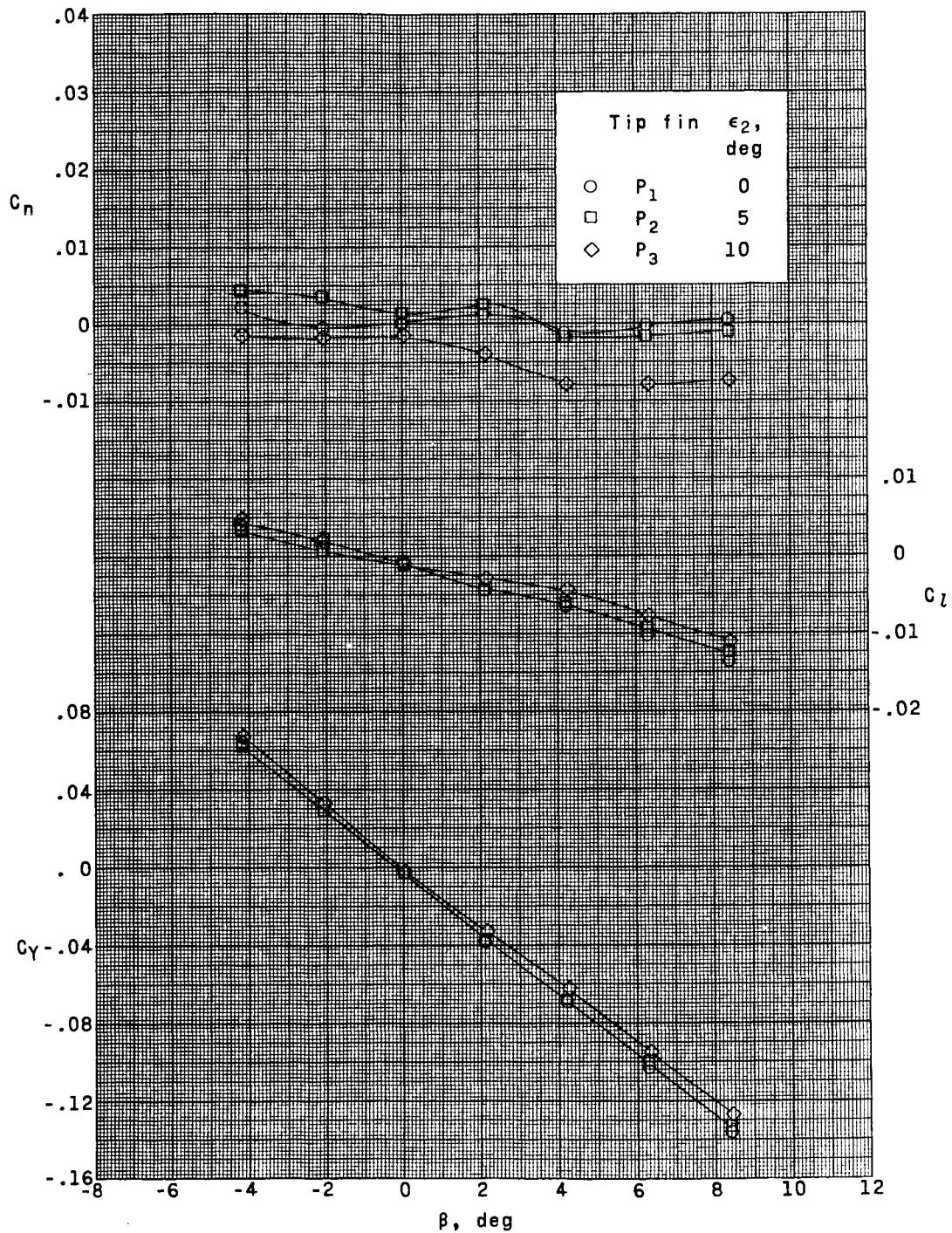
(a) $M = 1.50$.

Figure 5.- Effect of P_1 tip-fin toe-in angle on basic lateral characteristics in sideslip. $\alpha \approx 19^\circ$.



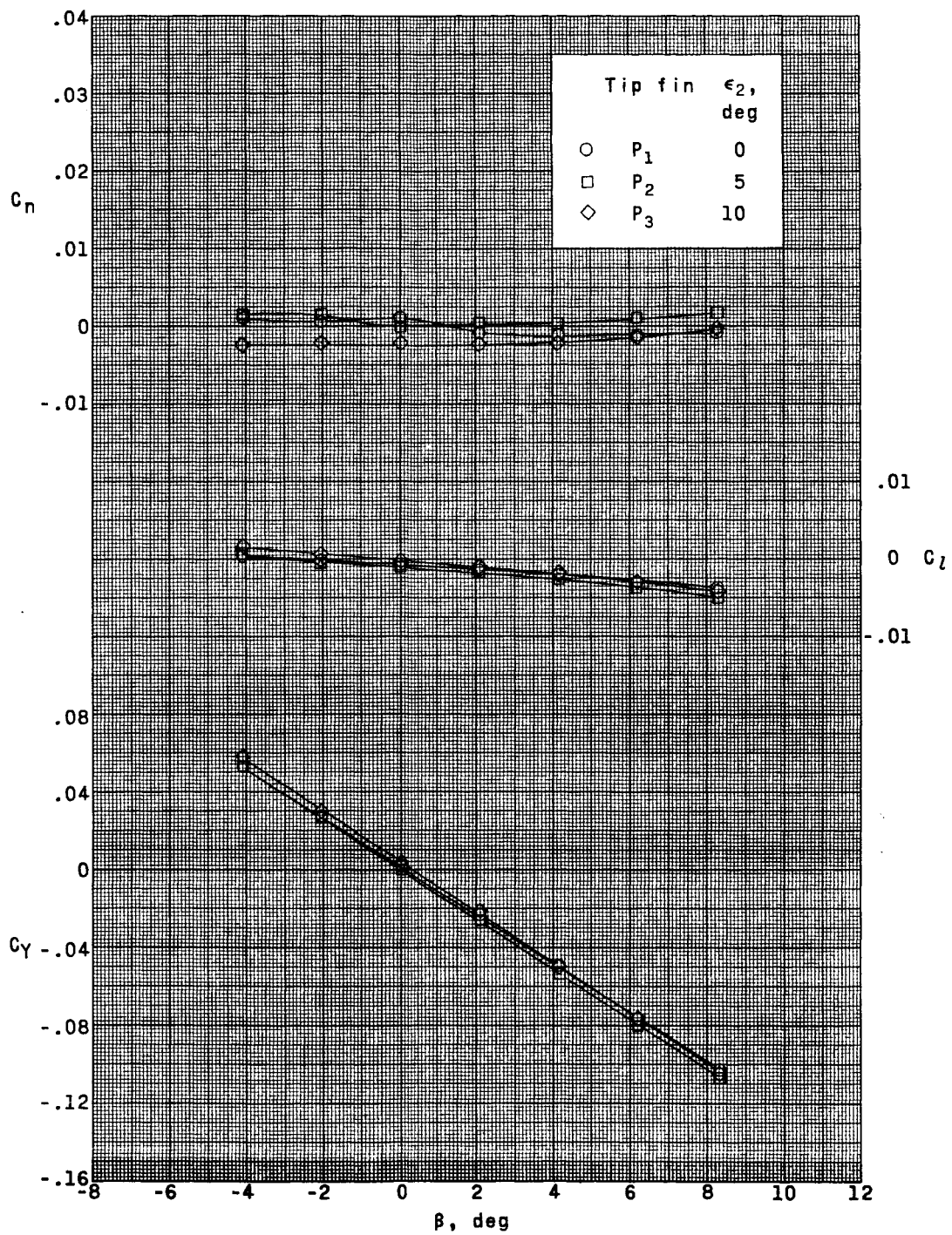
(b) $M = 2.86$.

Figure 5.- Concluded.



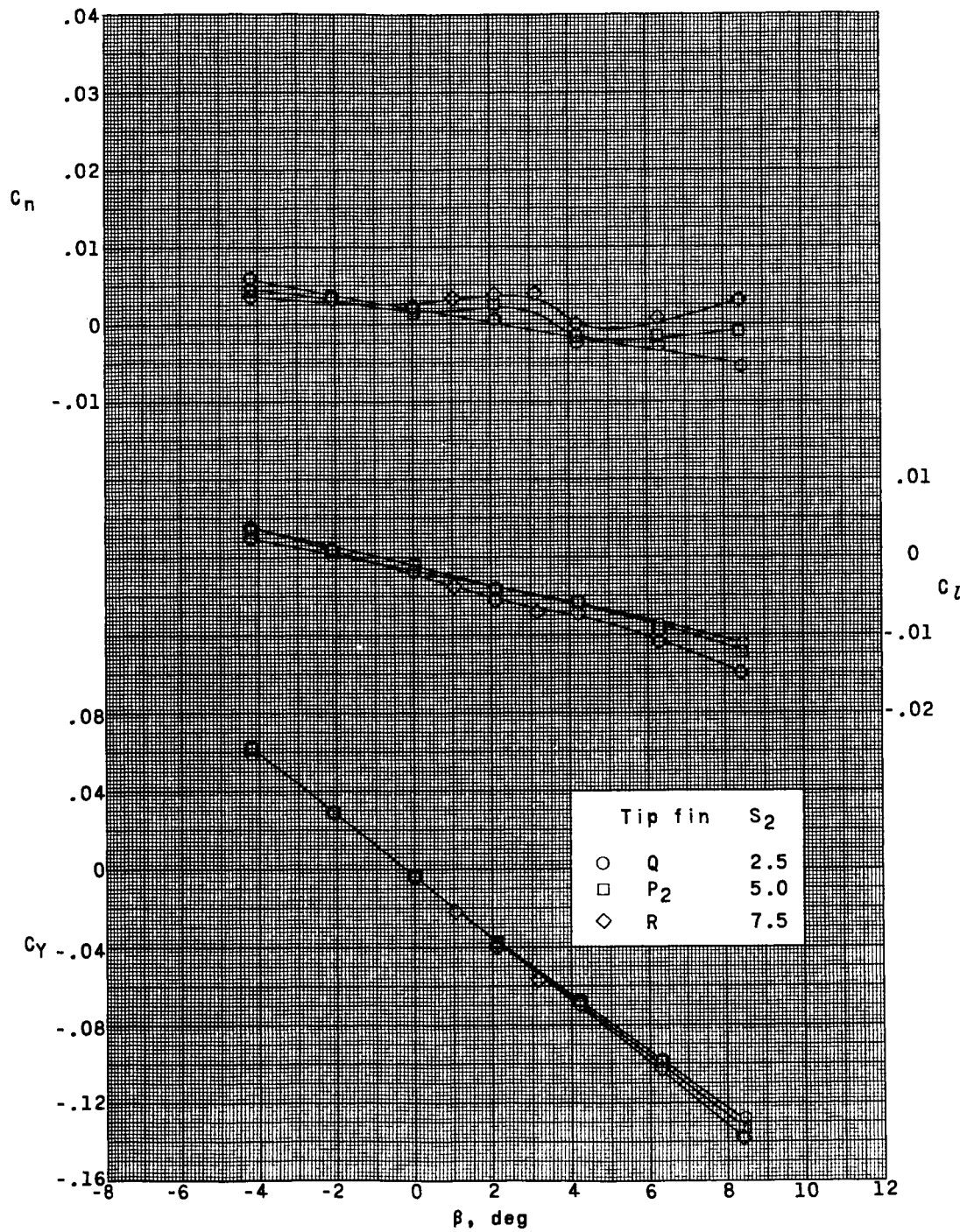
(a) $M = 1.50$.

Figure 6.- Effect of upper-panel toe-in angle (ϵ_2) on basic lateral characteristics in sideslip. $\alpha \approx 19^\circ$.



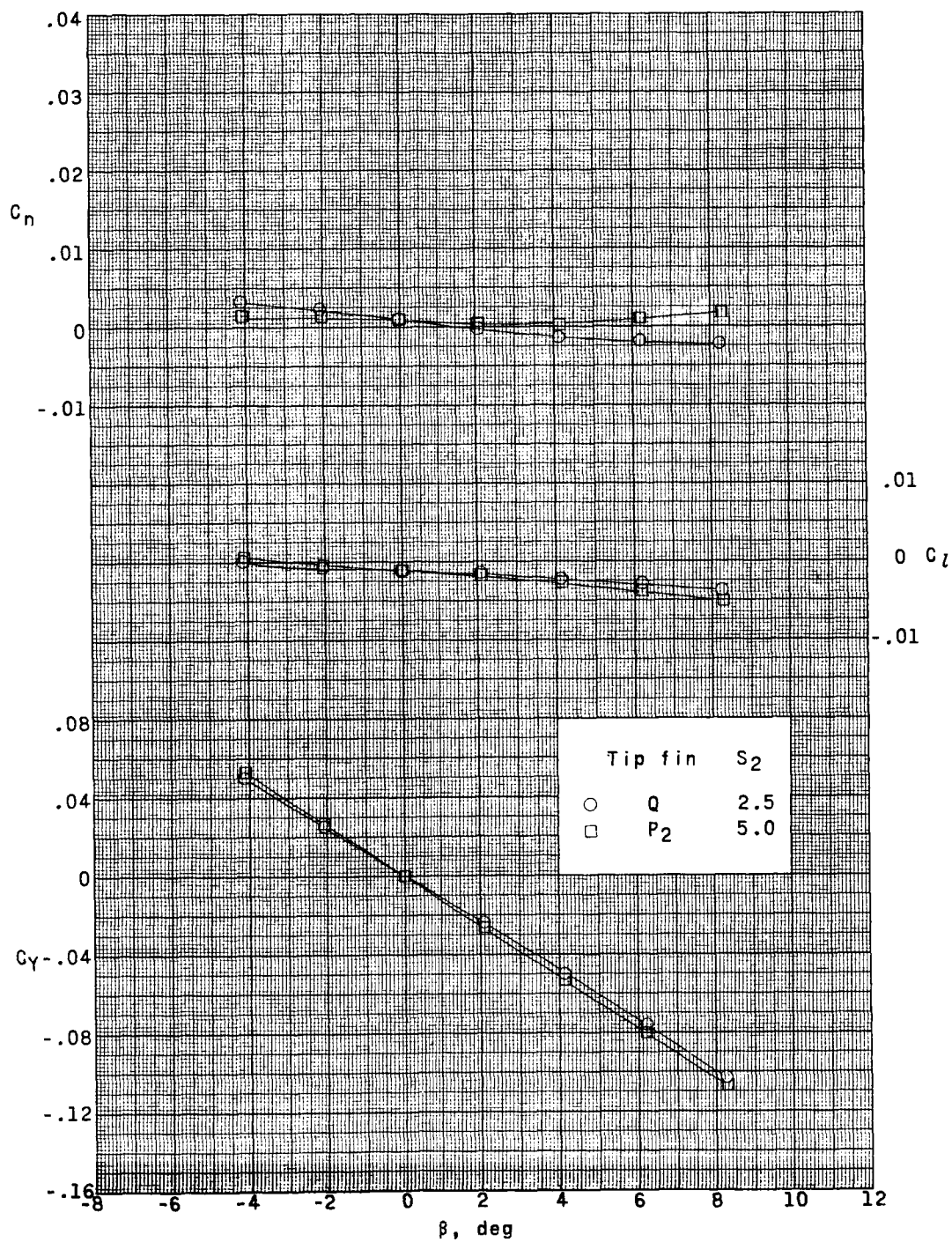
(b) $M = 2.86$.

Figure 6.- Concluded.



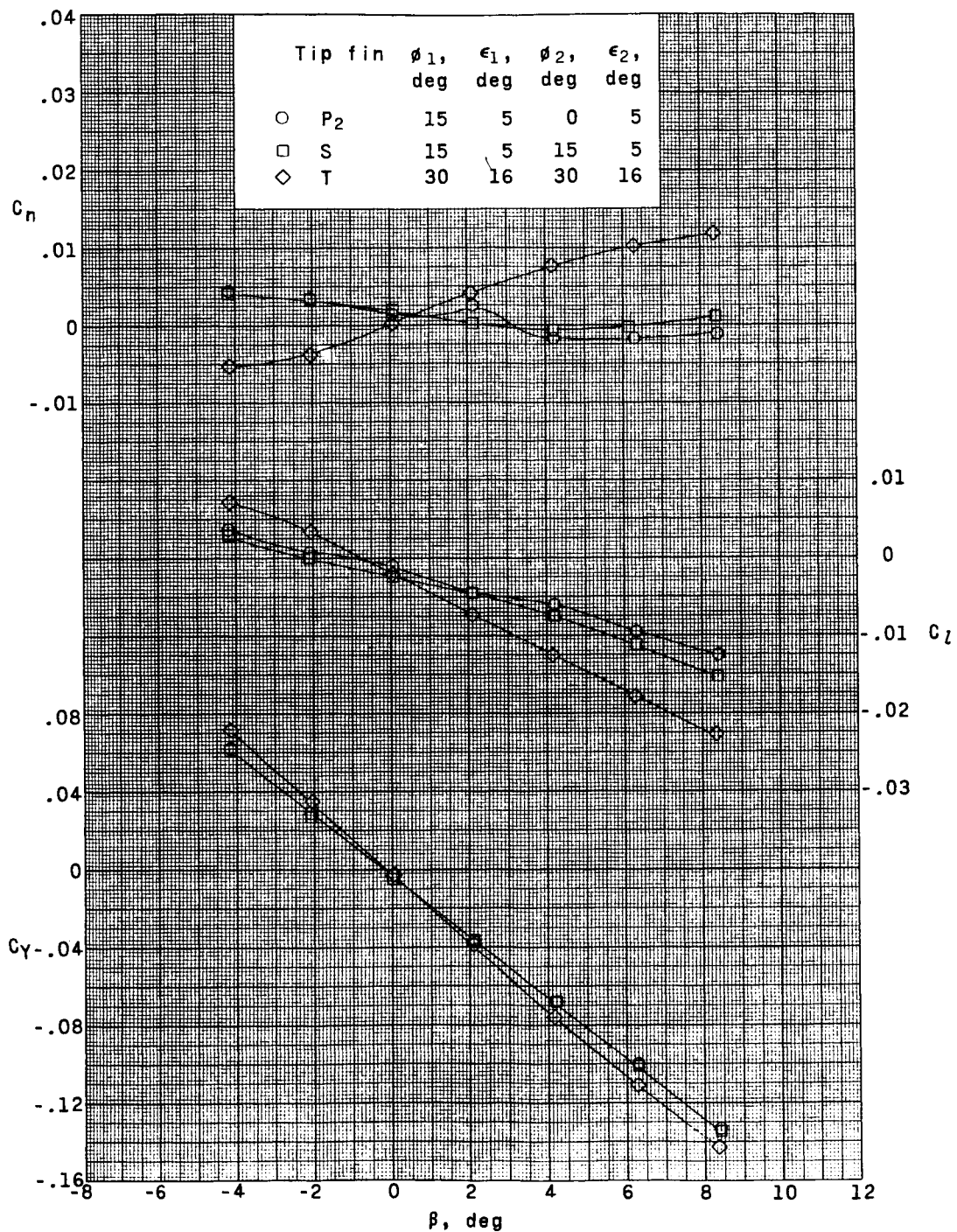
(a) $M = 1.50$.

Figure 7.- Effect of upper-panel planform area (S_2) on basic lateral characteristics in sideslip. $\alpha \approx 19^\circ$.



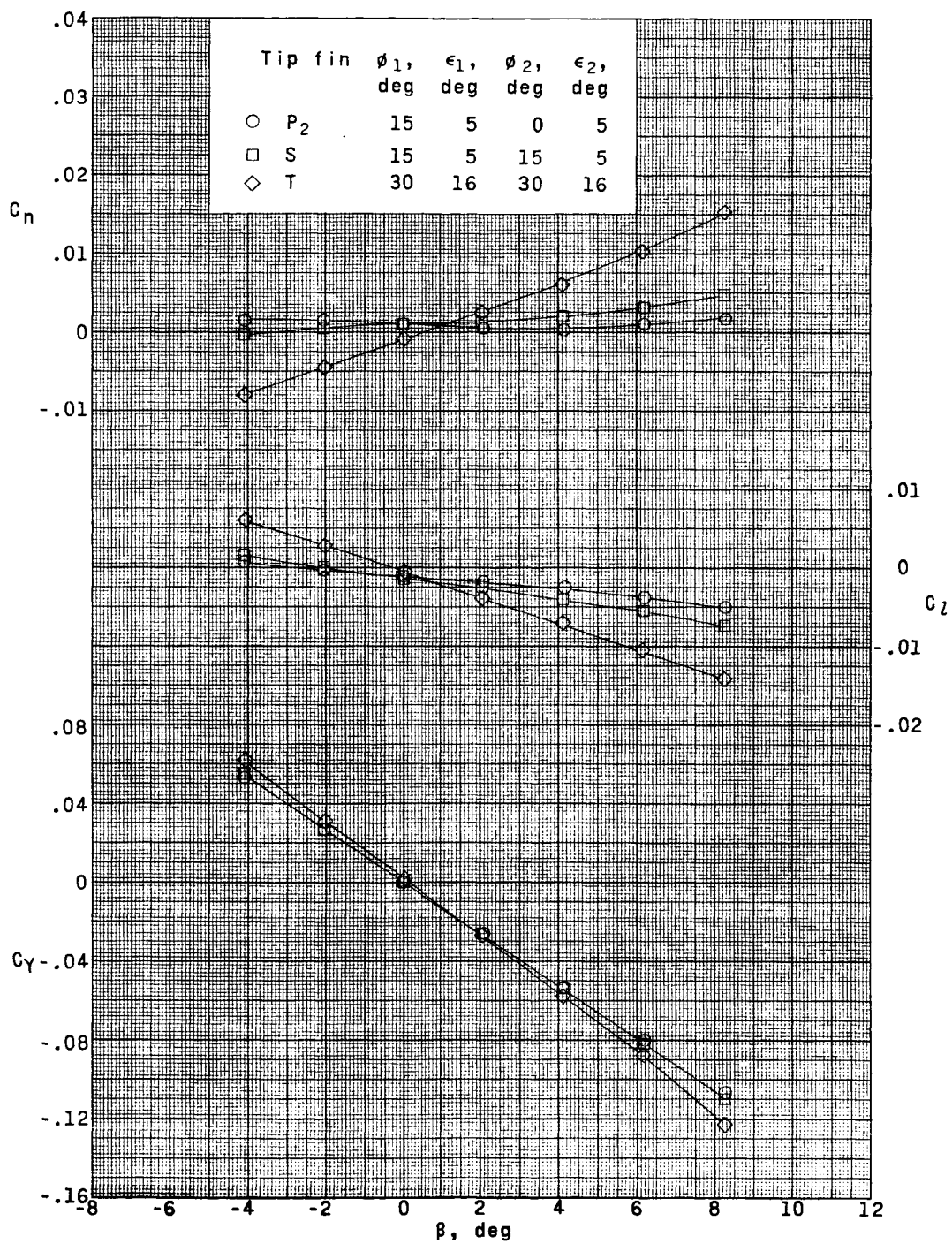
(b) $M = 2.86$.

Figure 7.- Concluded.



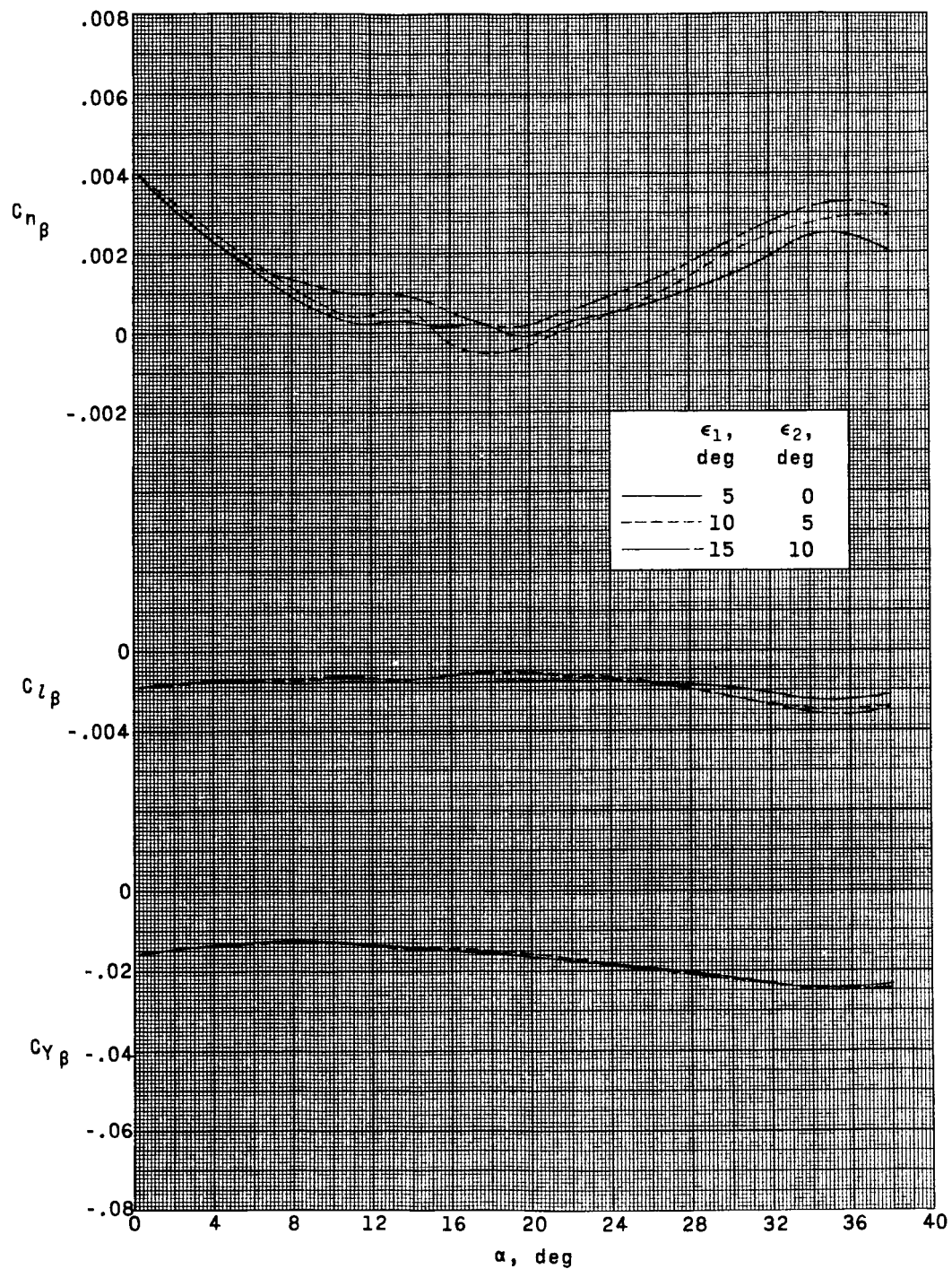
(a) $M = 1.50$.

Figure 8.- Effect of upper-panel roll-out angle (ϕ_2) on basic lateral characteristics in sideslip. $\alpha \approx 19^\circ$.



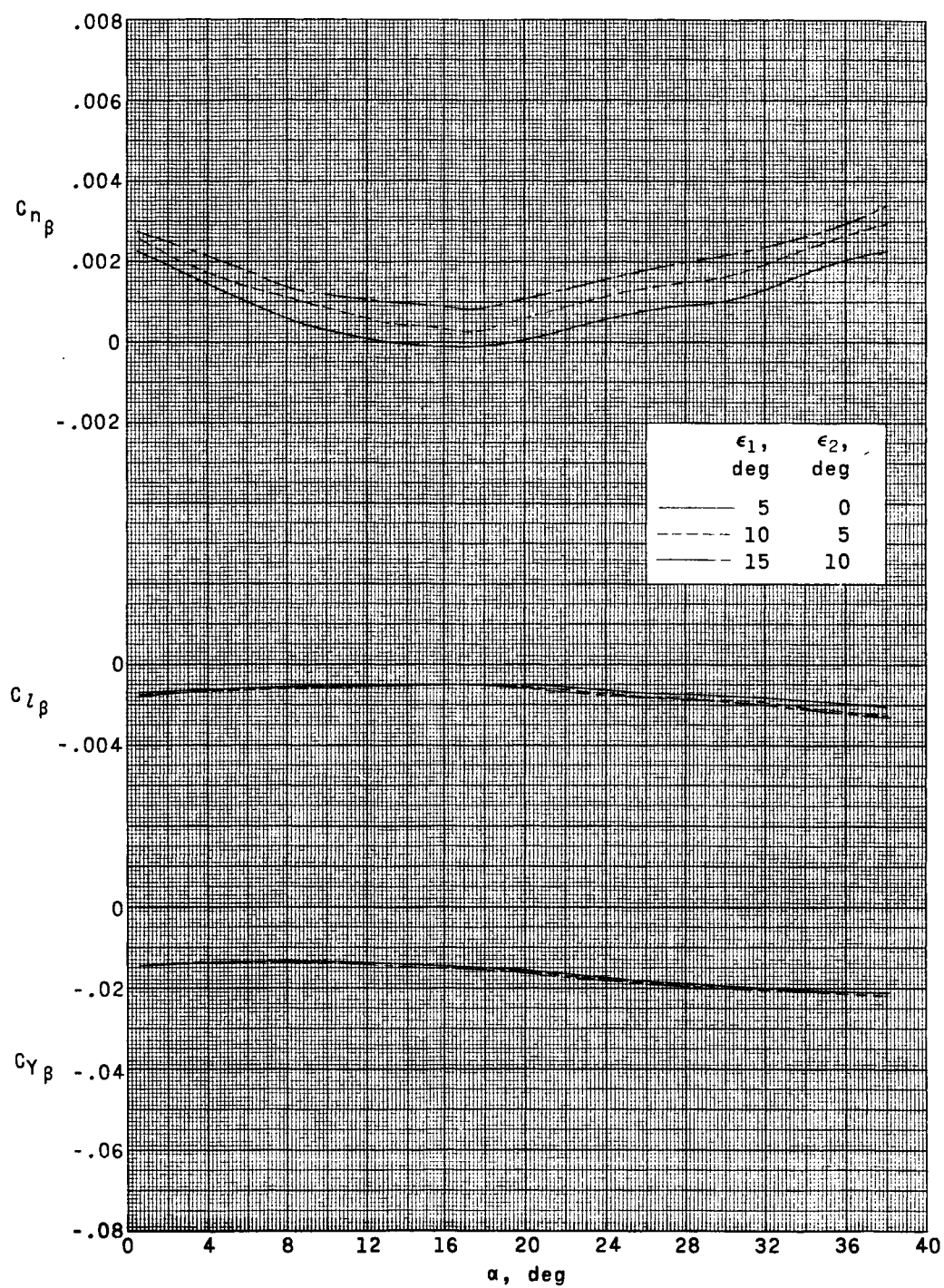
(b) $M = 2.86$.

Figure 8.- Concluded.



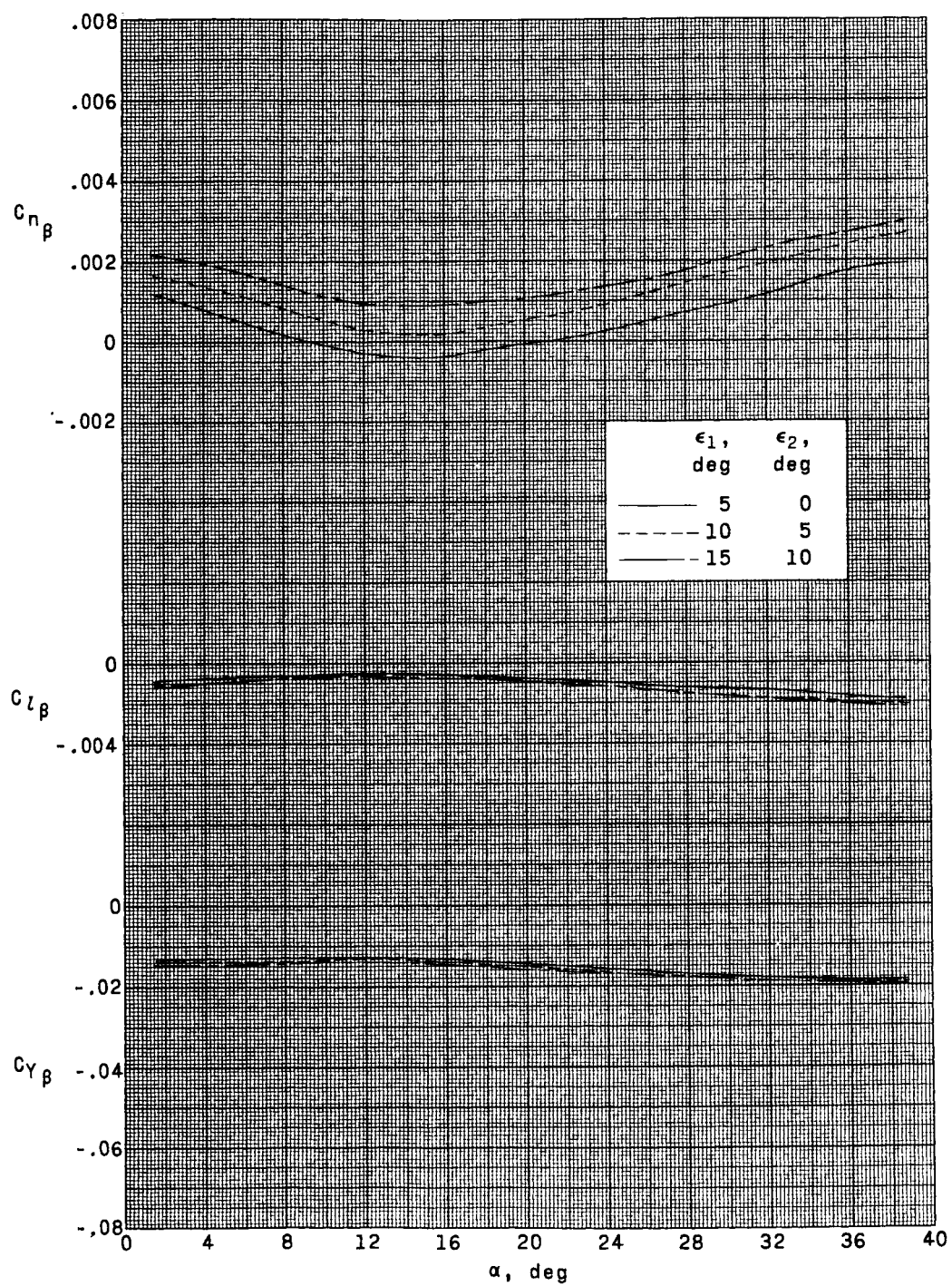
(a) $M = 1.50$.

Figure 9.- Effect of P_1 tip-fin toe-in angle on the variation of the sideslip parameters with angle of attack.



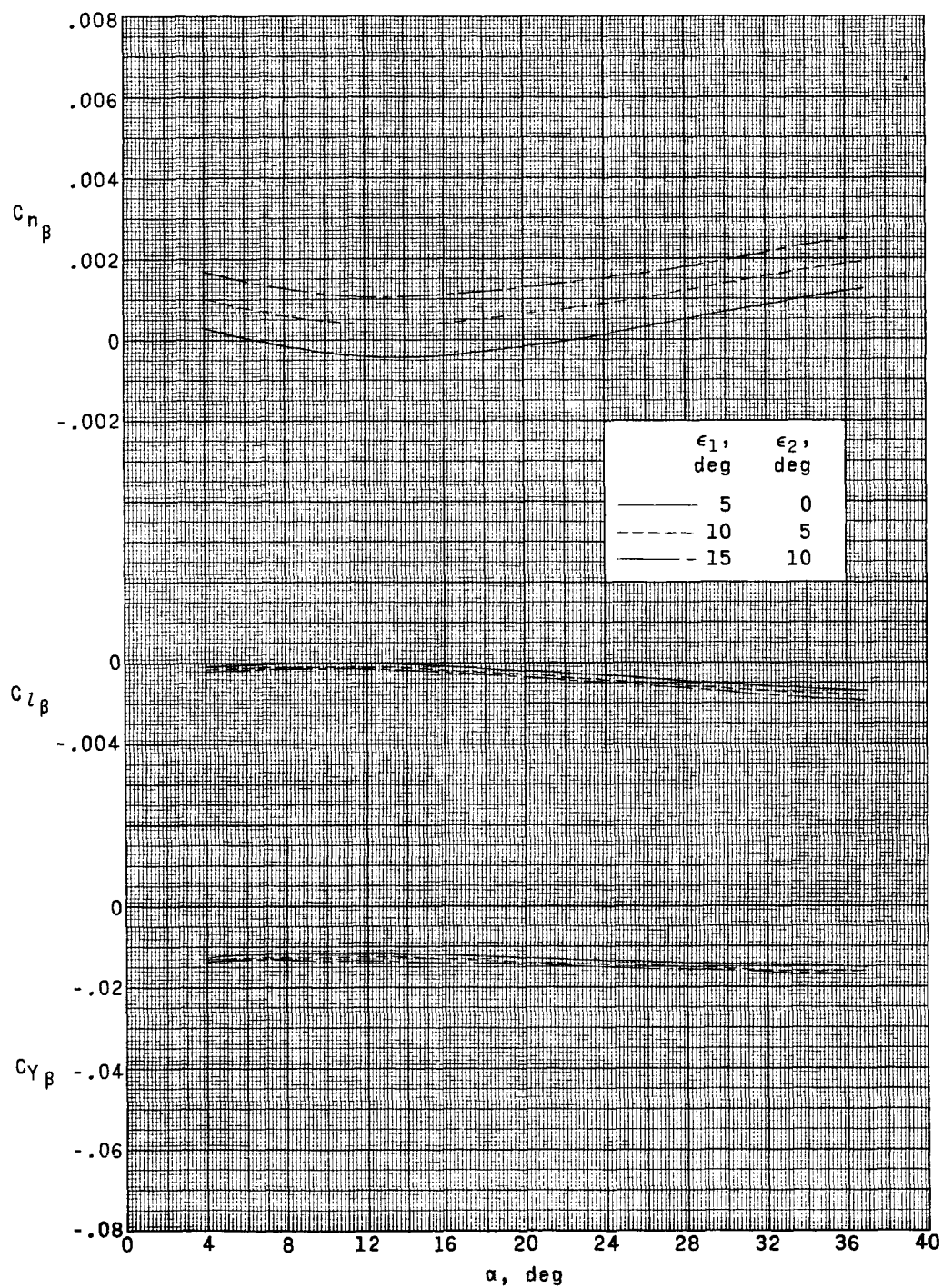
(b) $M = 1.80$.

Figure 9.- Continued.



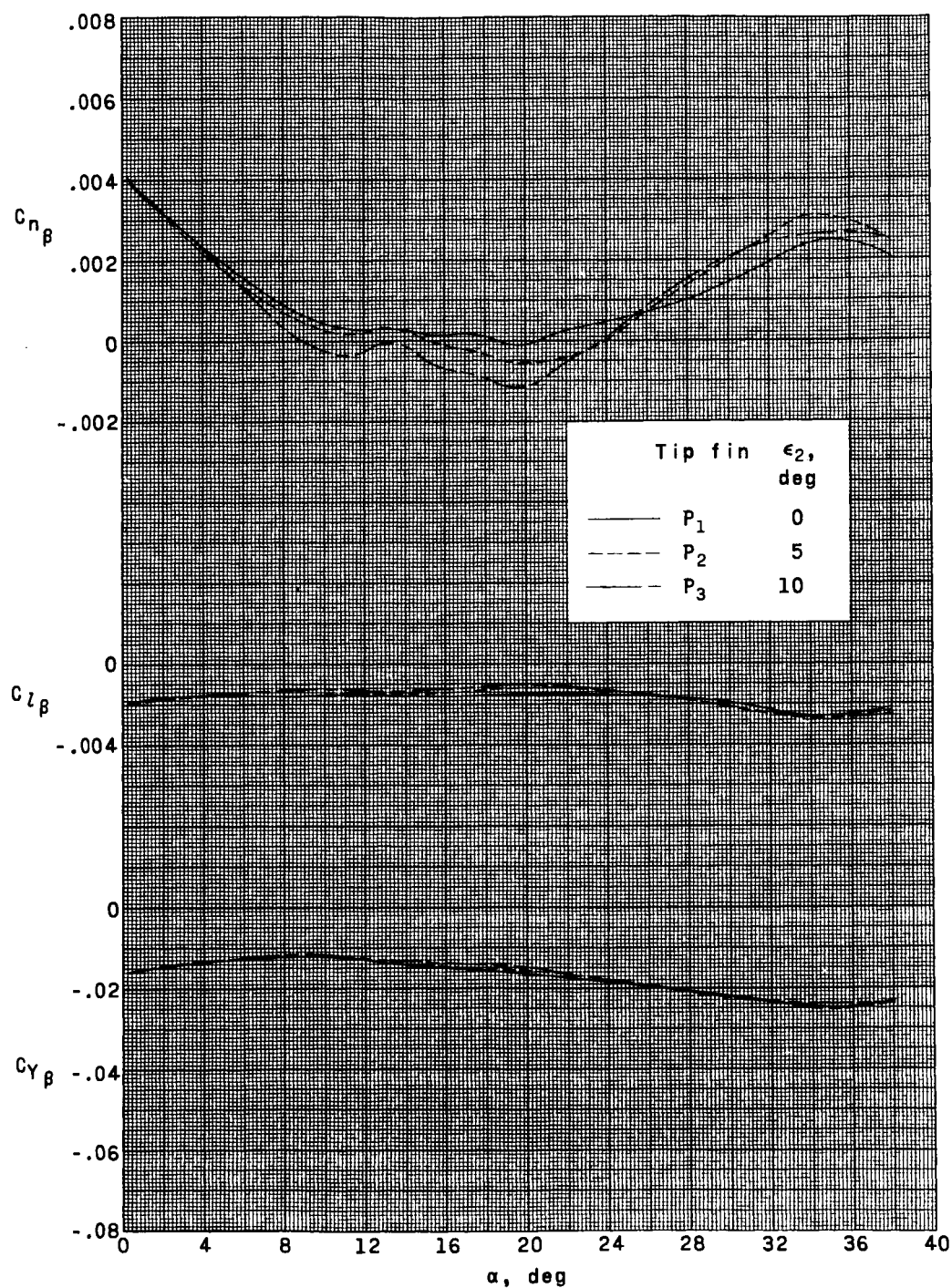
(c) $M = 2.16$.

Figure 9.- Continued.



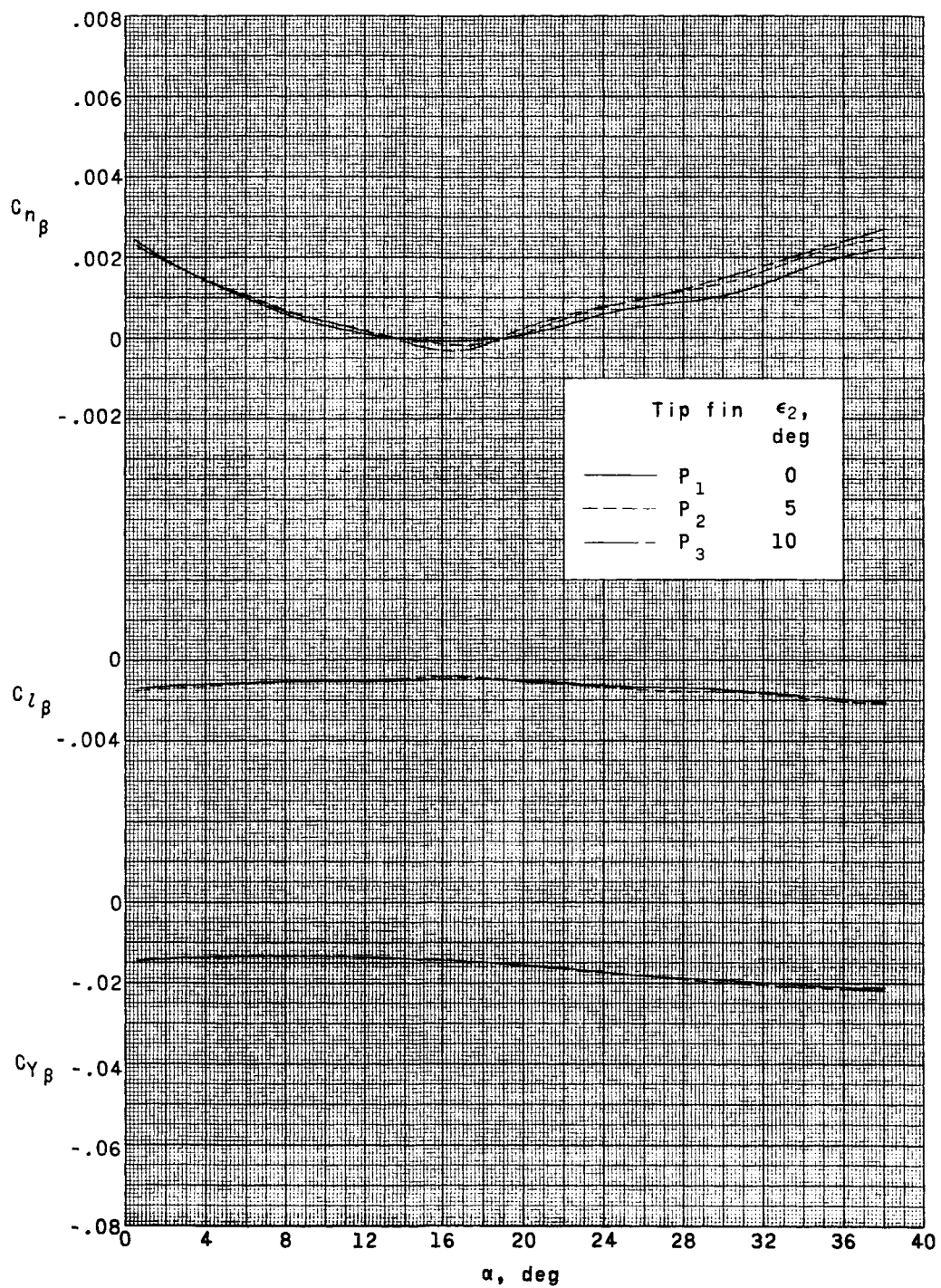
(d) $M = 2.86$.

Figure 9.- Concluded.



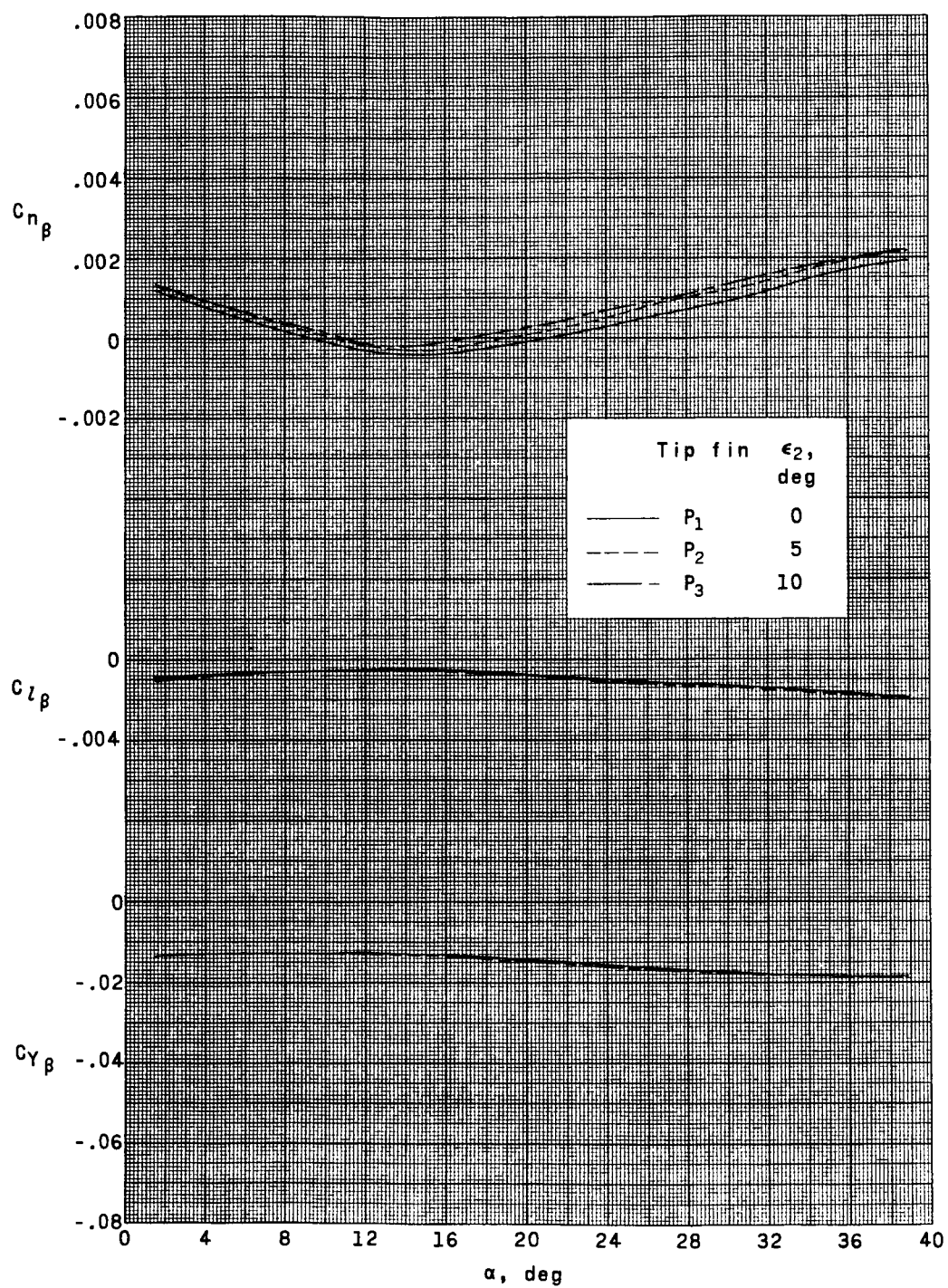
(a) $M = 1.50$.

Figure 10.- Effect of upper-panel toe-in angle (ϵ_2) on the variation of the sideslip parameters with angle of attack.



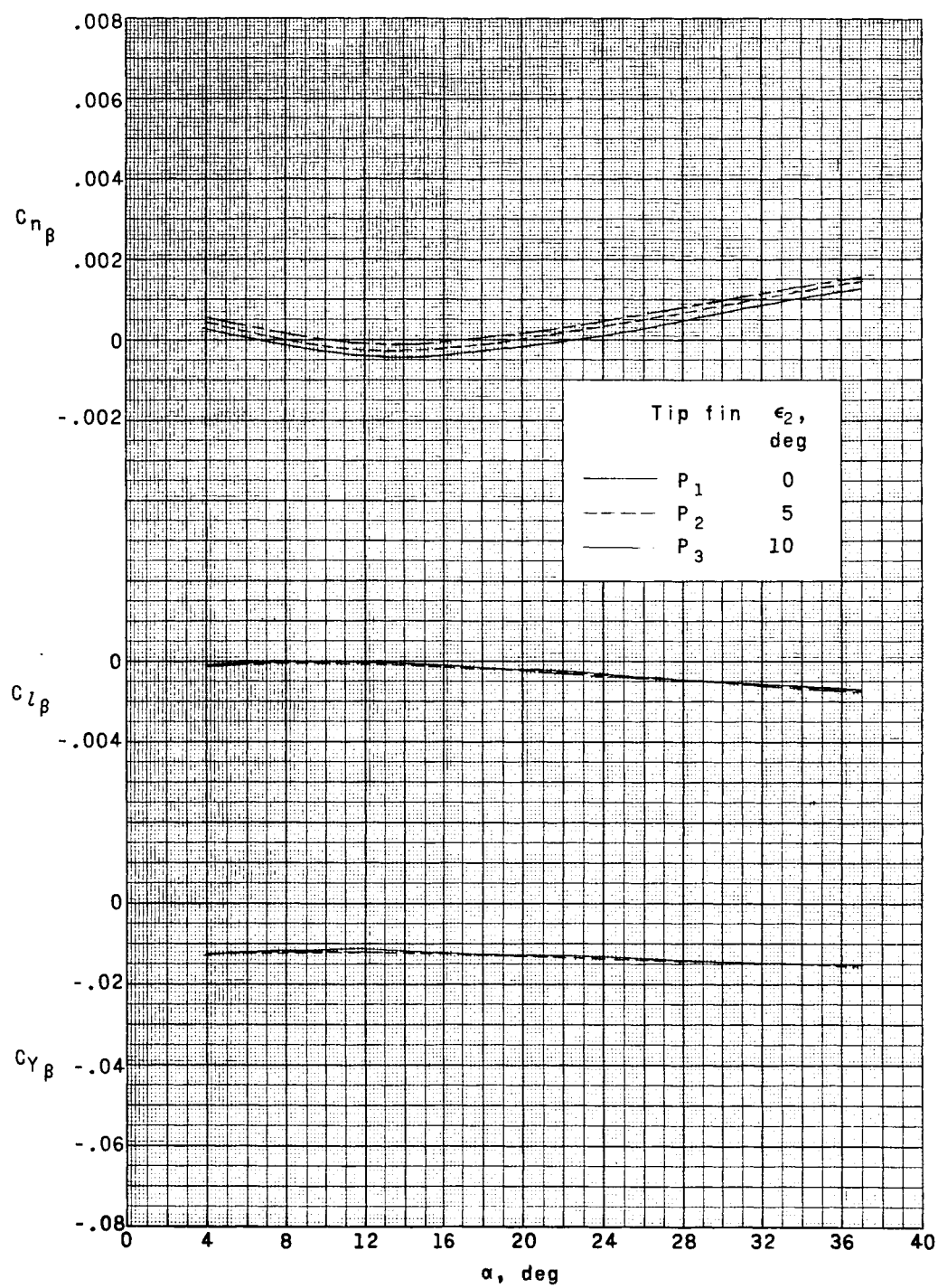
(b) $M = 1.80$.

Figure 10.- Continued.



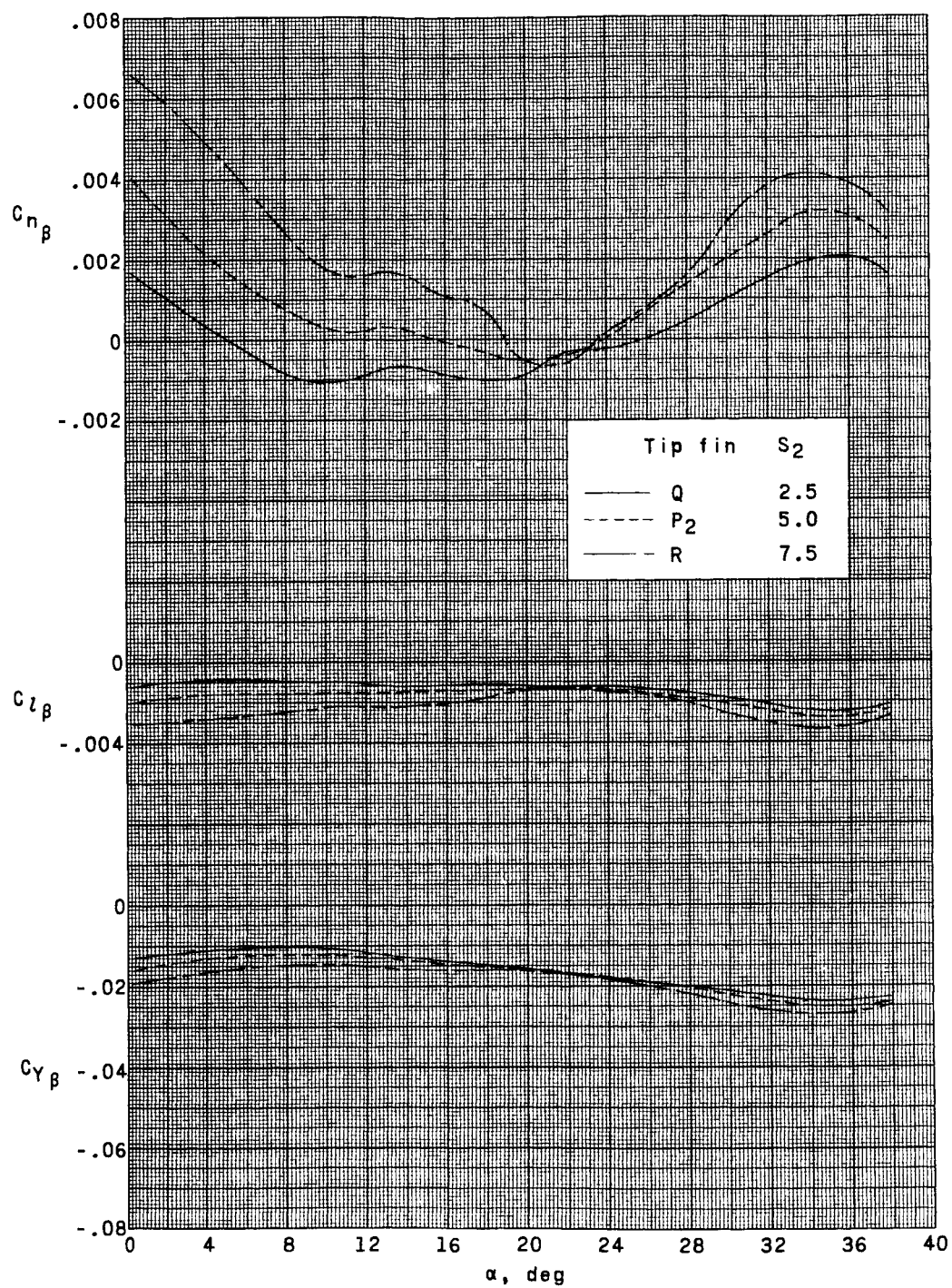
(c) $M = 2.16$.

Figure 10.- Continued.



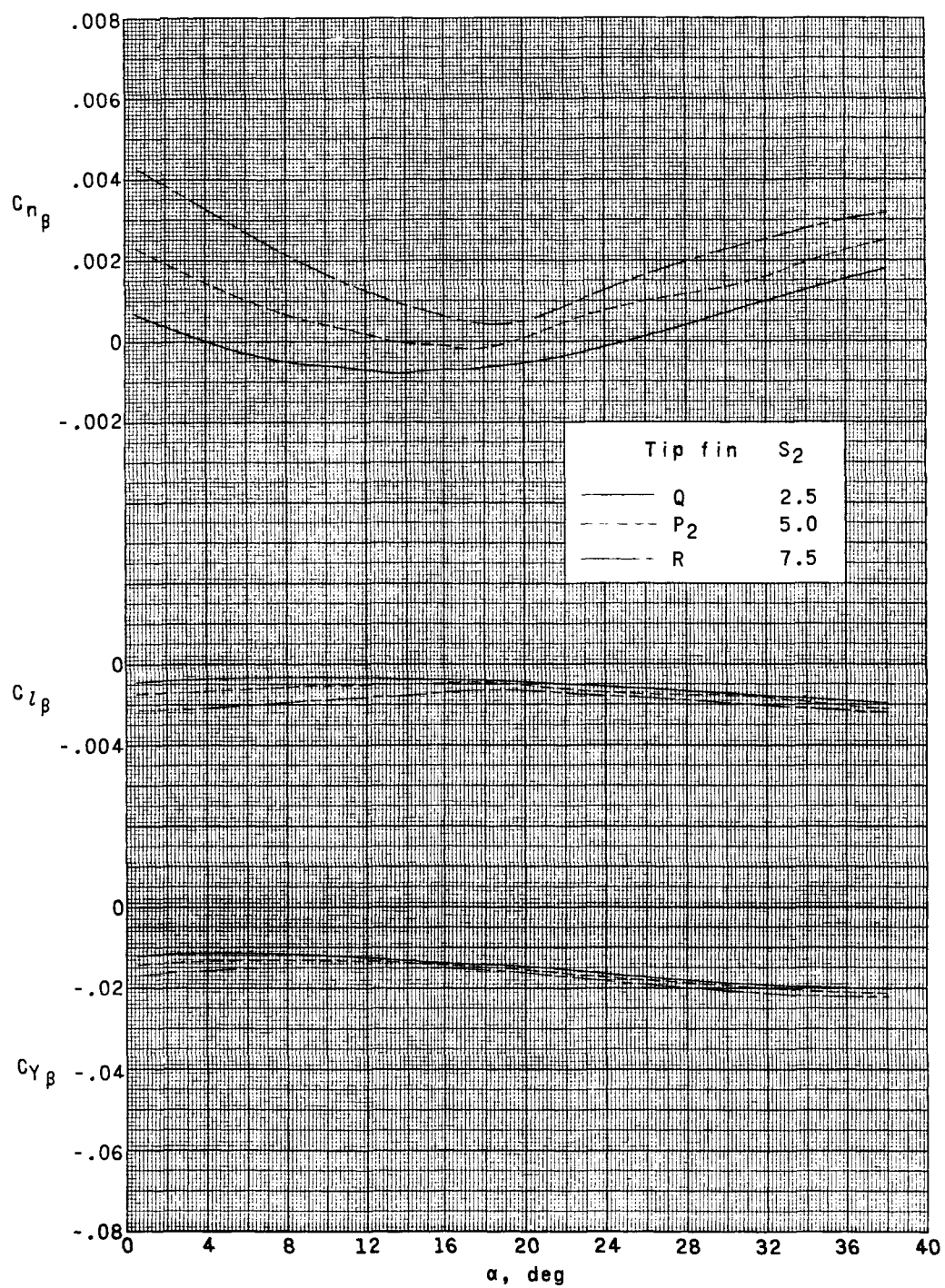
(d) $M = 2.86$.

Figure 10.- Concluded.



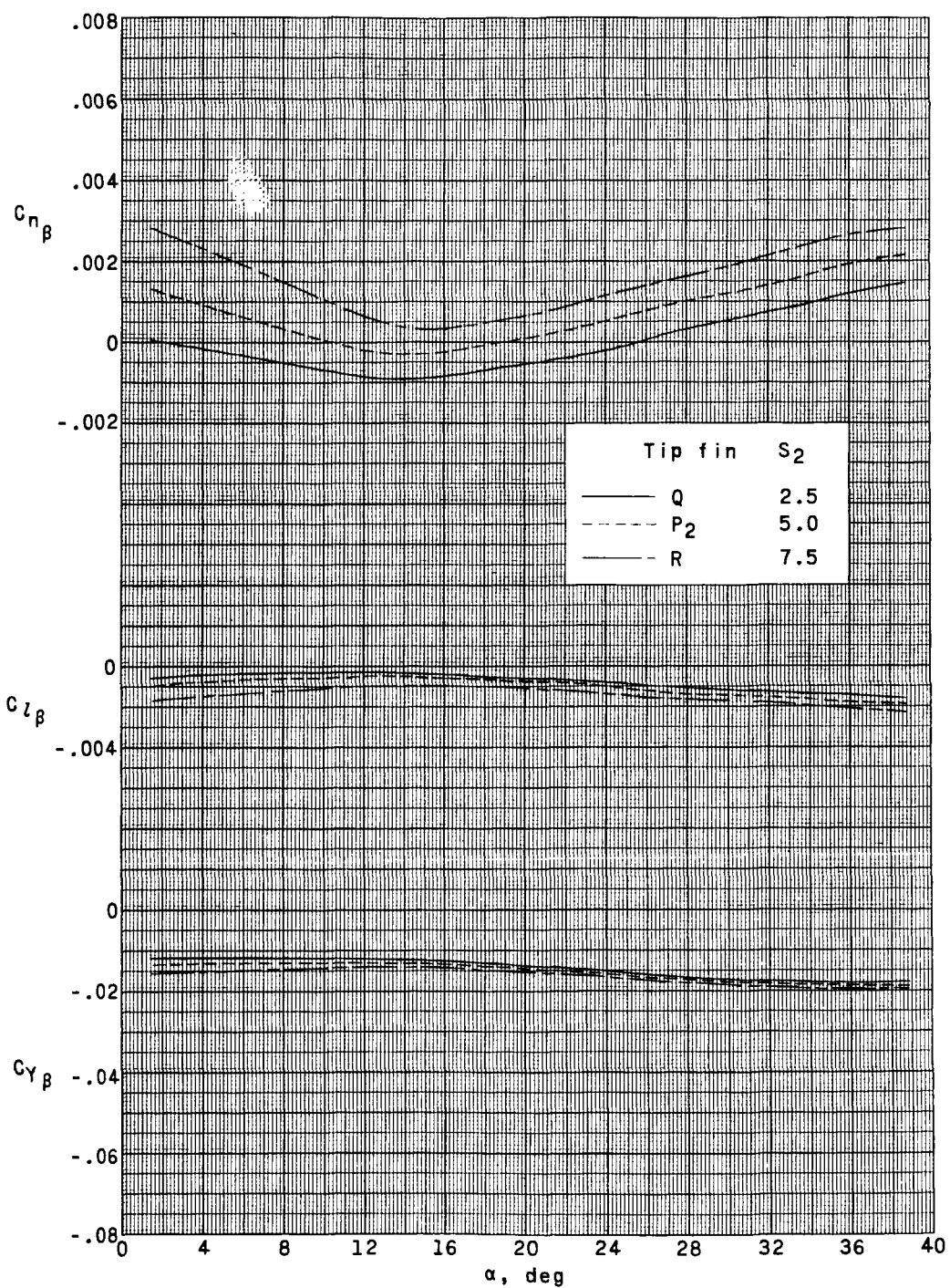
(a) $M = 1.50$.

Figure 11.- Effect of upper-panel planform area (S_2) on the variation of the sideslip parameters with angle of attack.



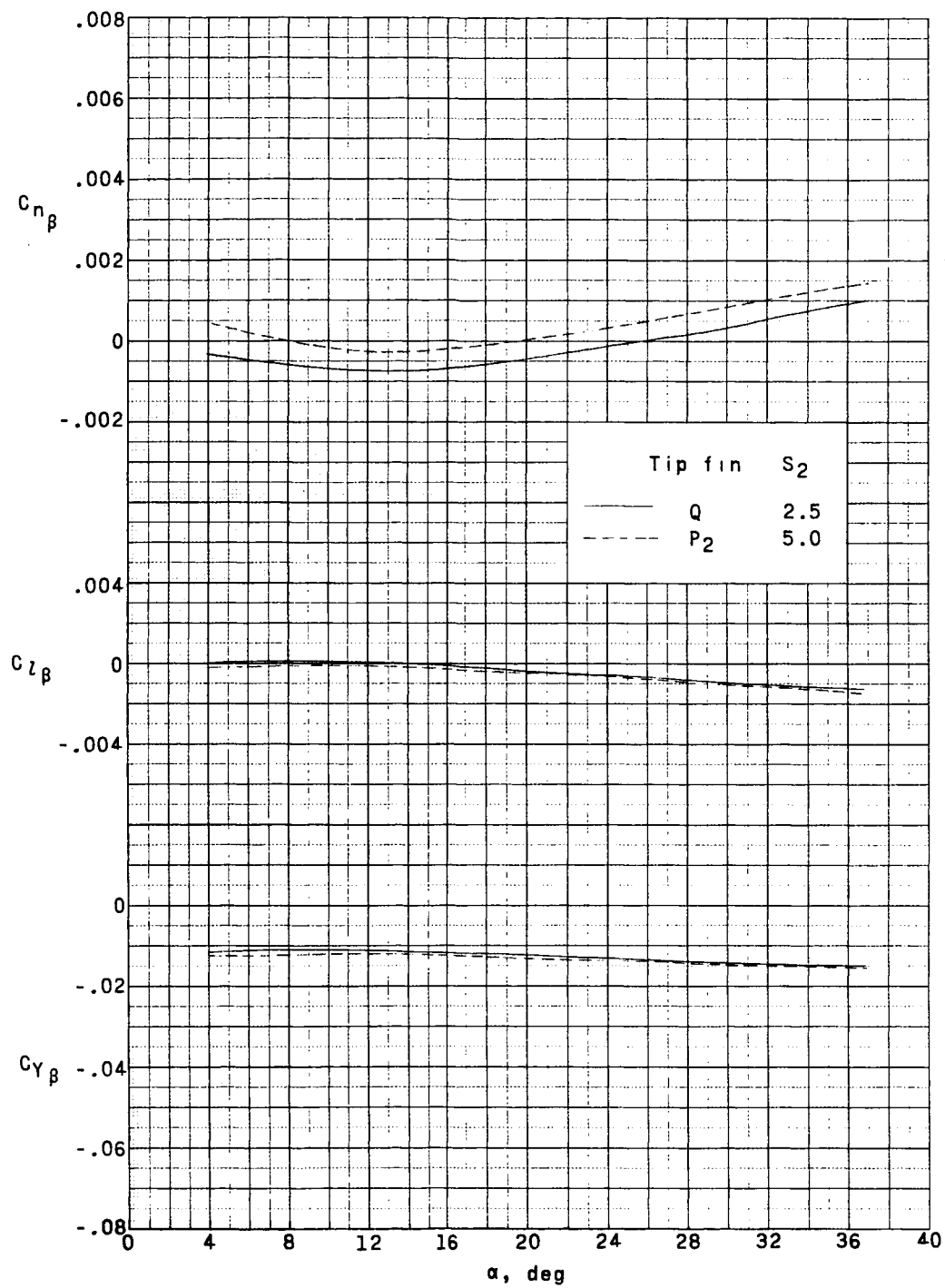
(b) $M = 1.80$.

Figure 11.- Continued.



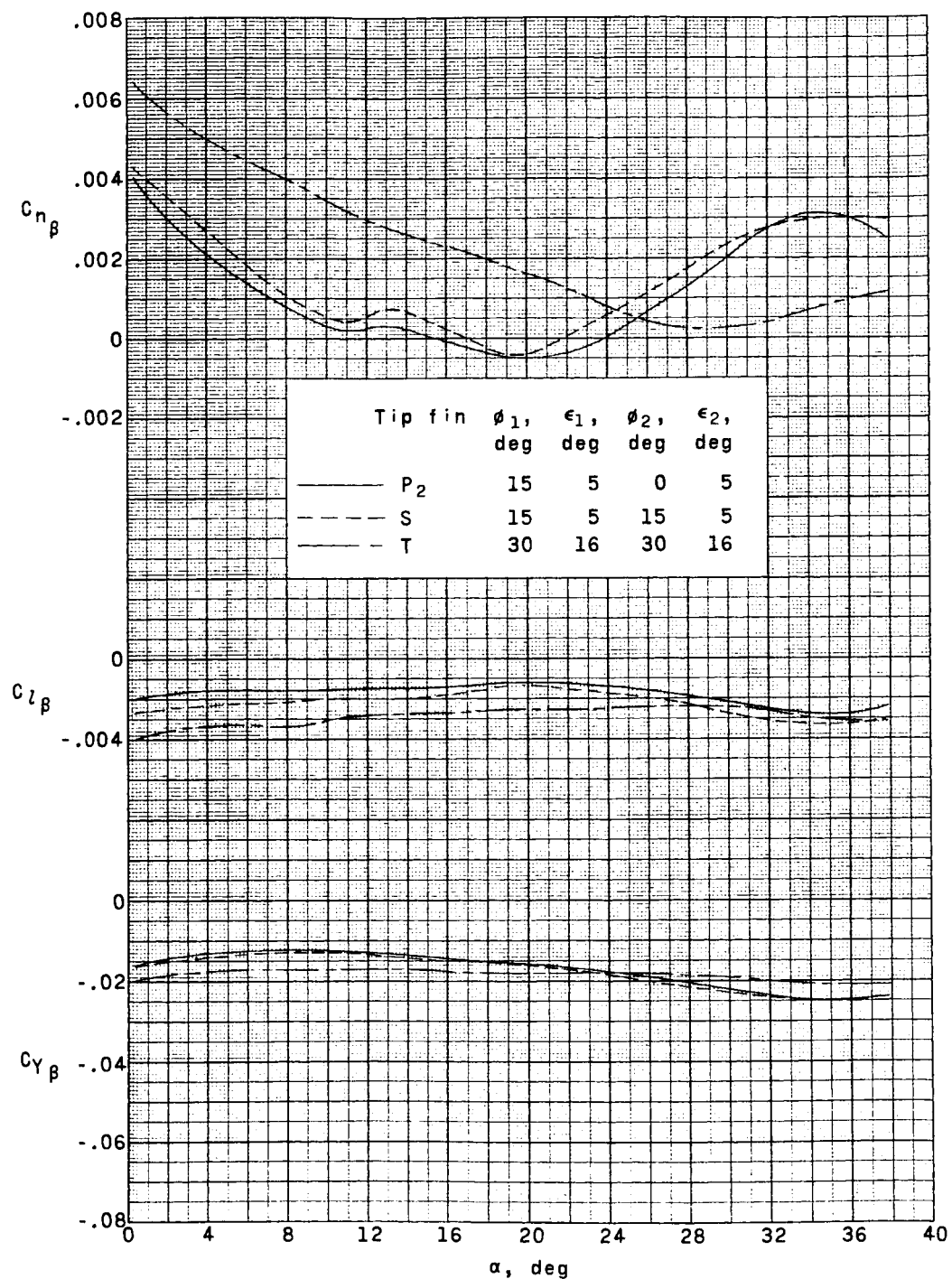
(c) $M = 2.16$.

Figure 11.- Continued.



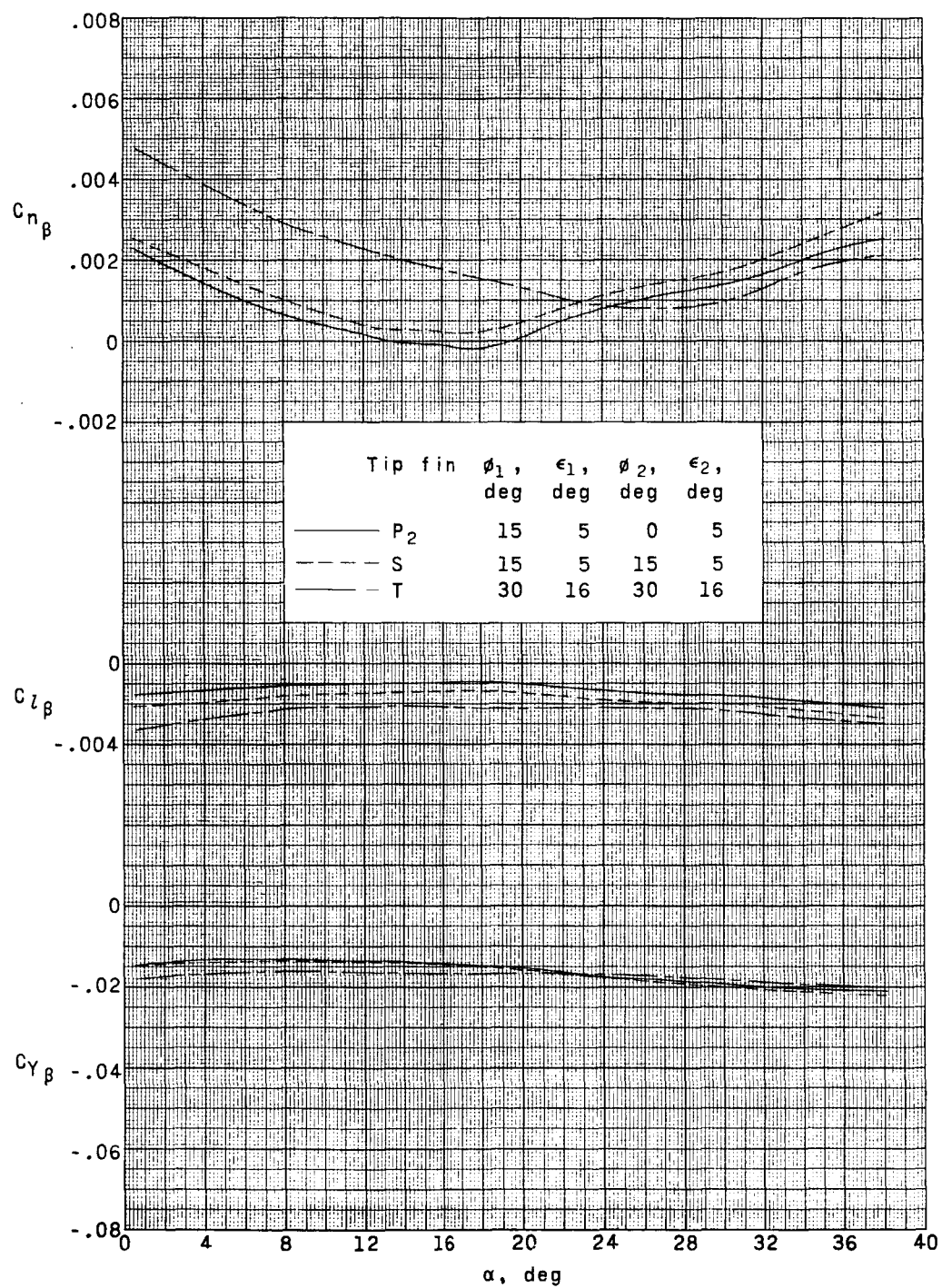
(d) $M = 2.86$.

Figure 11.- Concluded.



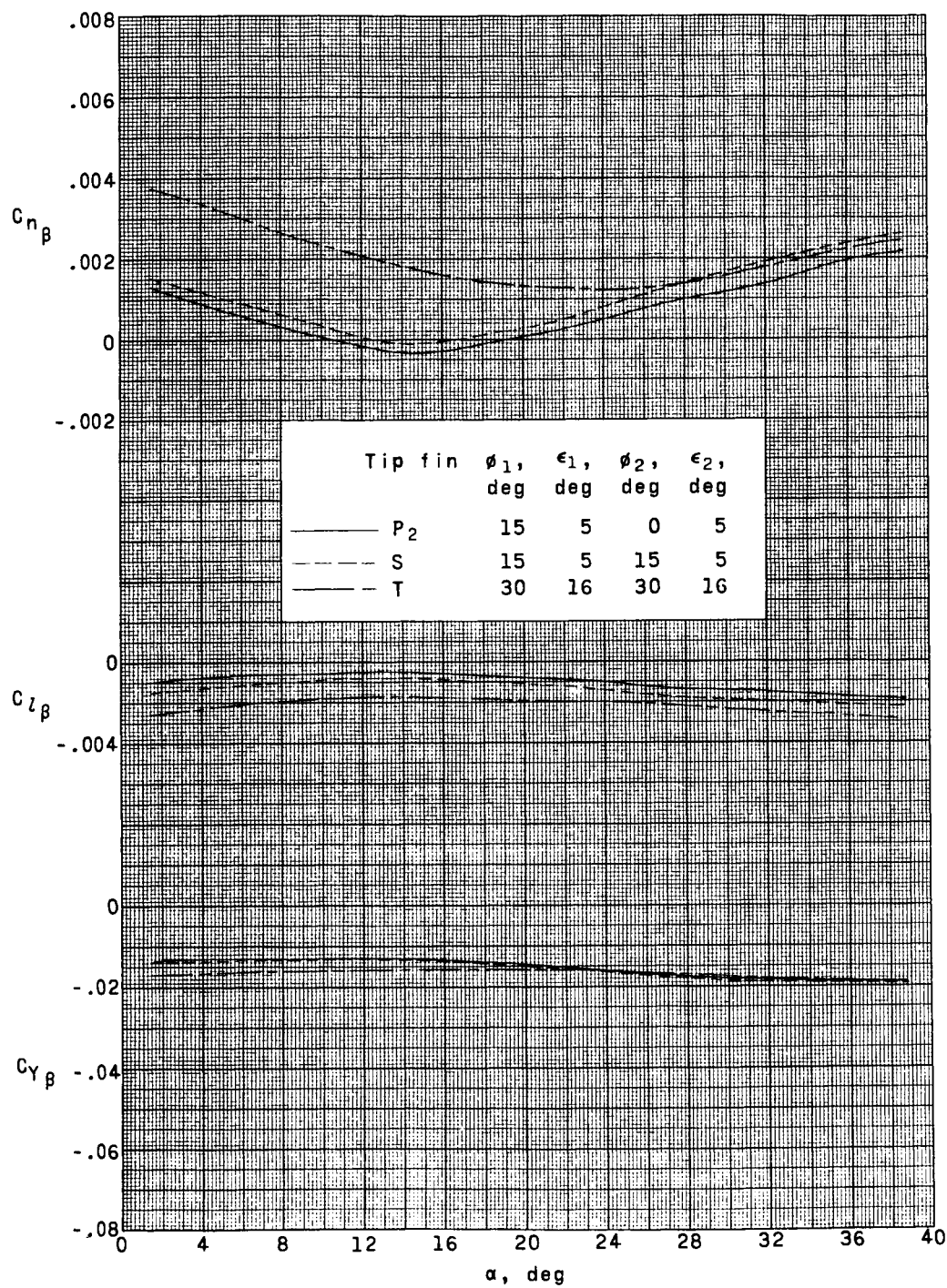
(a) $M = 1.50$.

Figure 12.- Effect of upper-panel roll-out angle (ϕ_2) on the variation of the sideslip parameters with angle of attack.



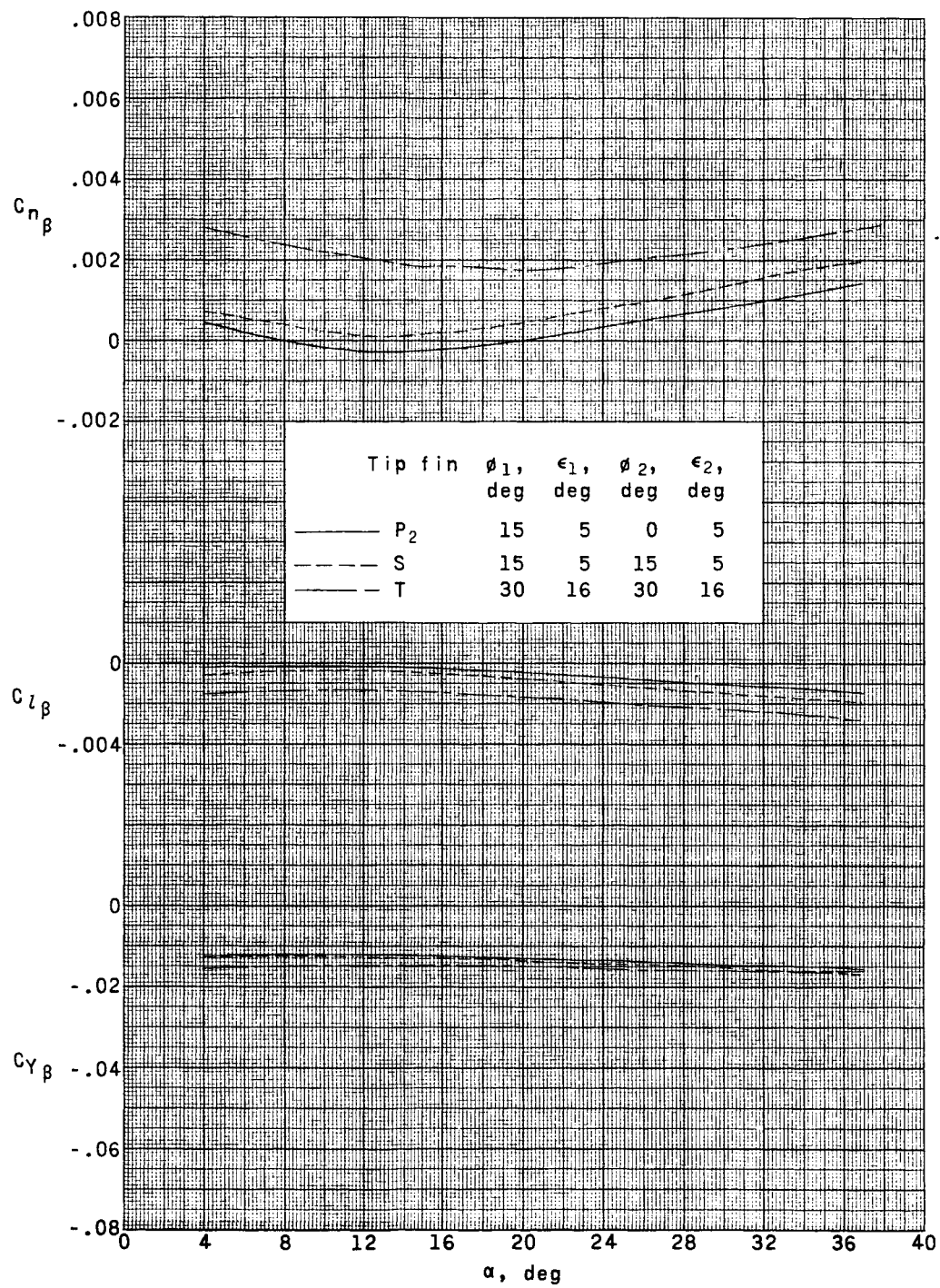
(b) $M = 1.80$.

Figure 12.- Continued.



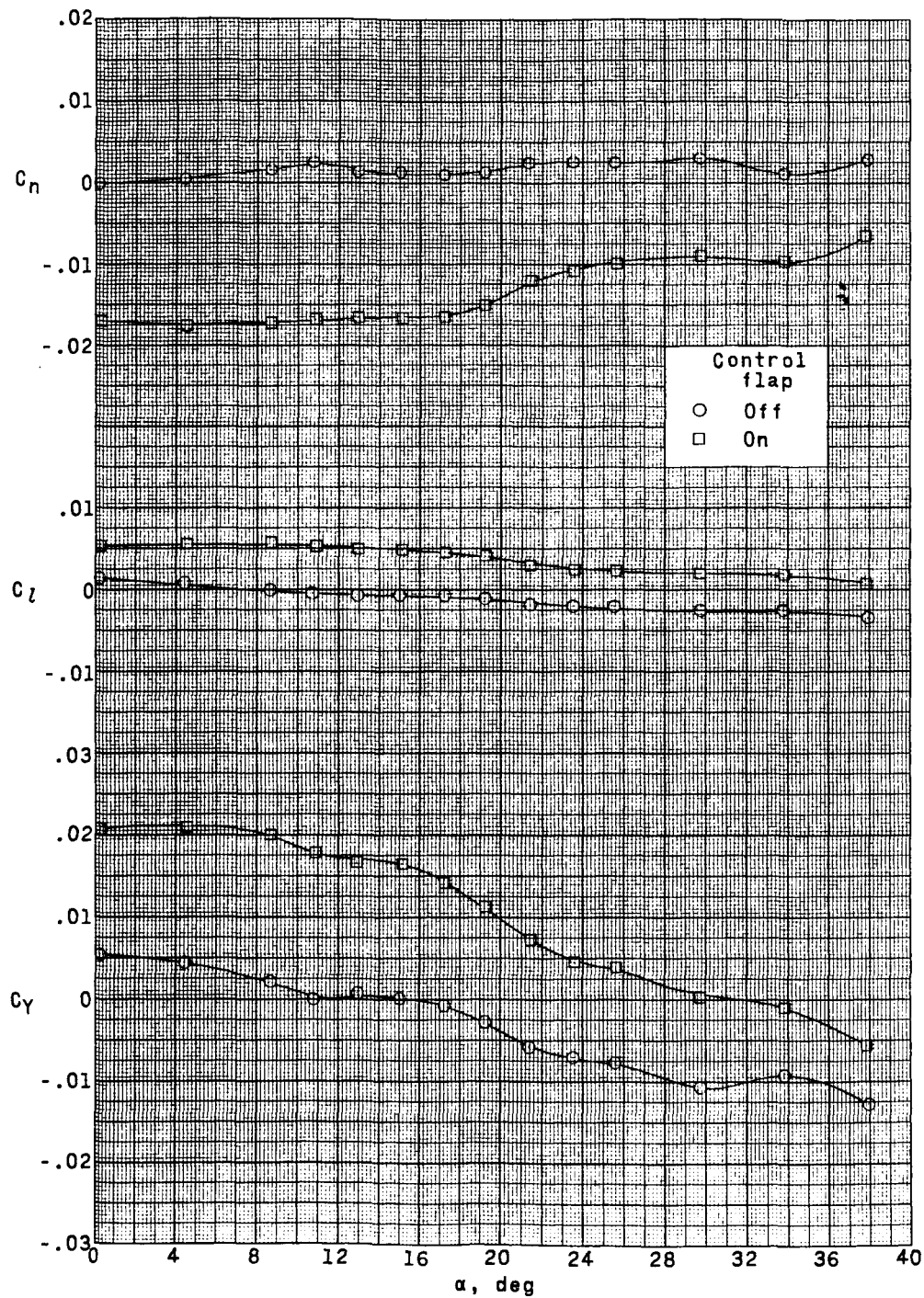
(c) $M = 2.16$.

Figure 12.- Continued.



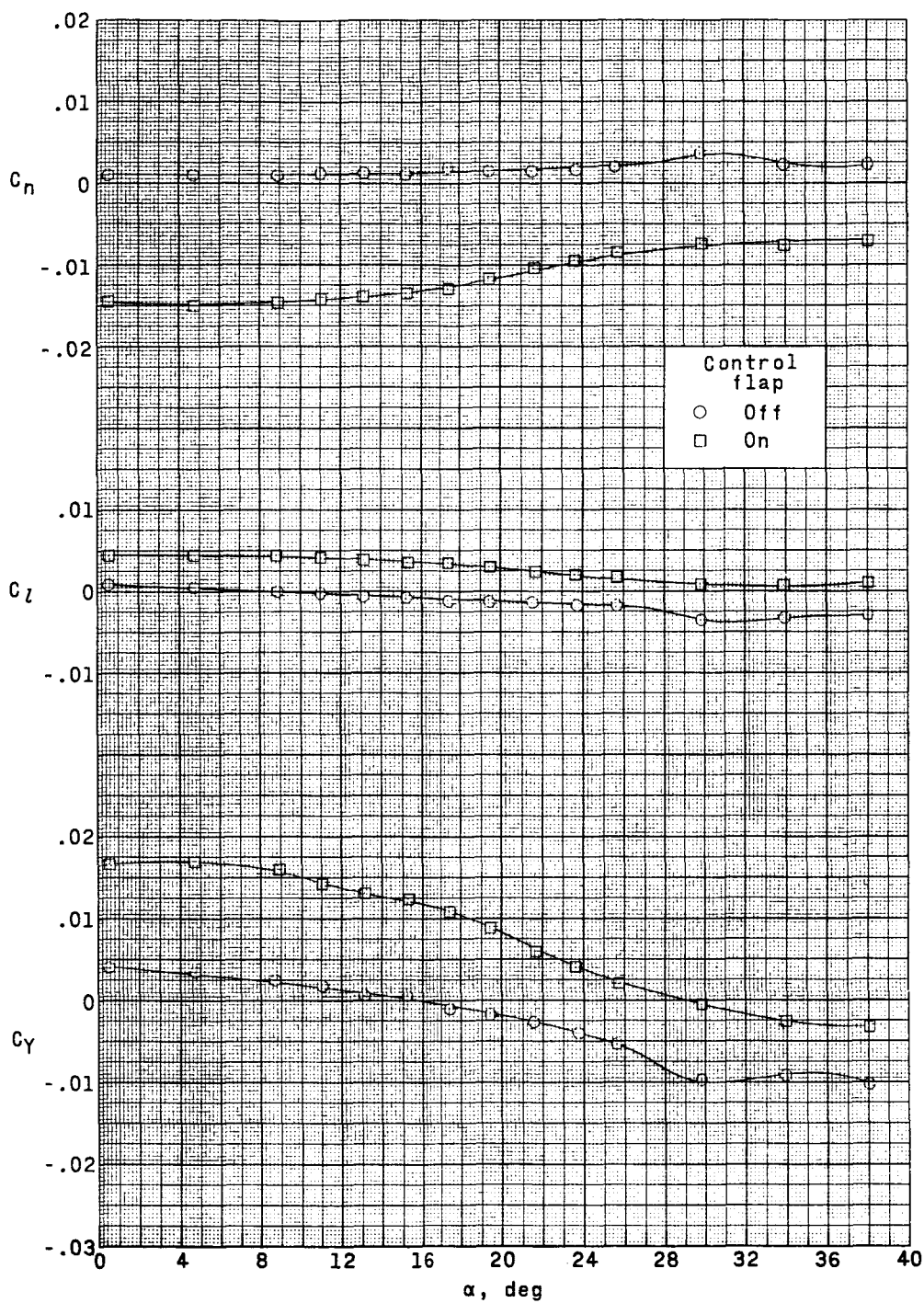
(d) $M = 2.86$.

Figure 12.- Concluded.



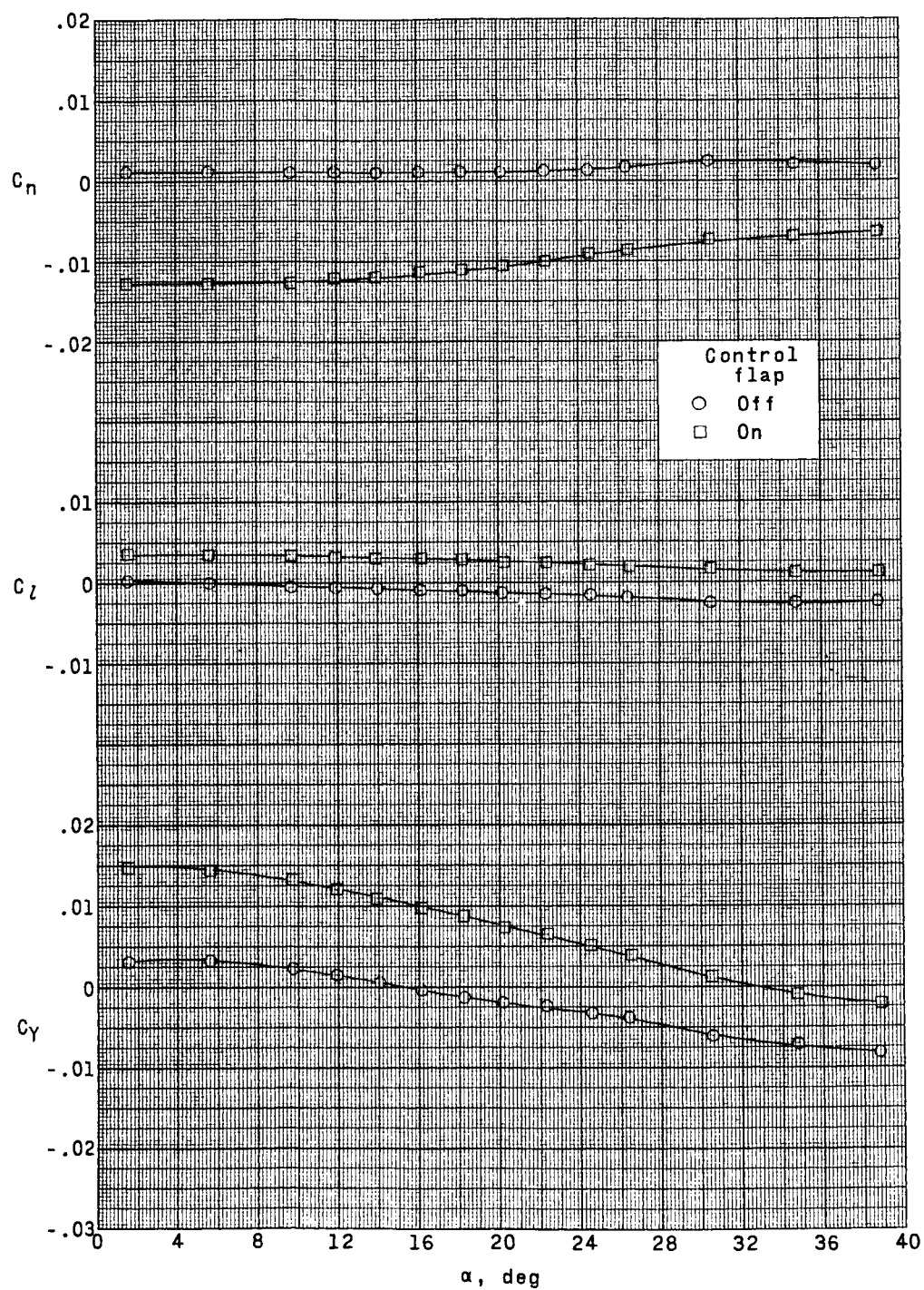
(a) $M = 1.50$.

Figure 13.- Effect of P_2 left tip-fin upper-panel control-surface deflection on the variation of the basic lateral characteristics with angle of attack.



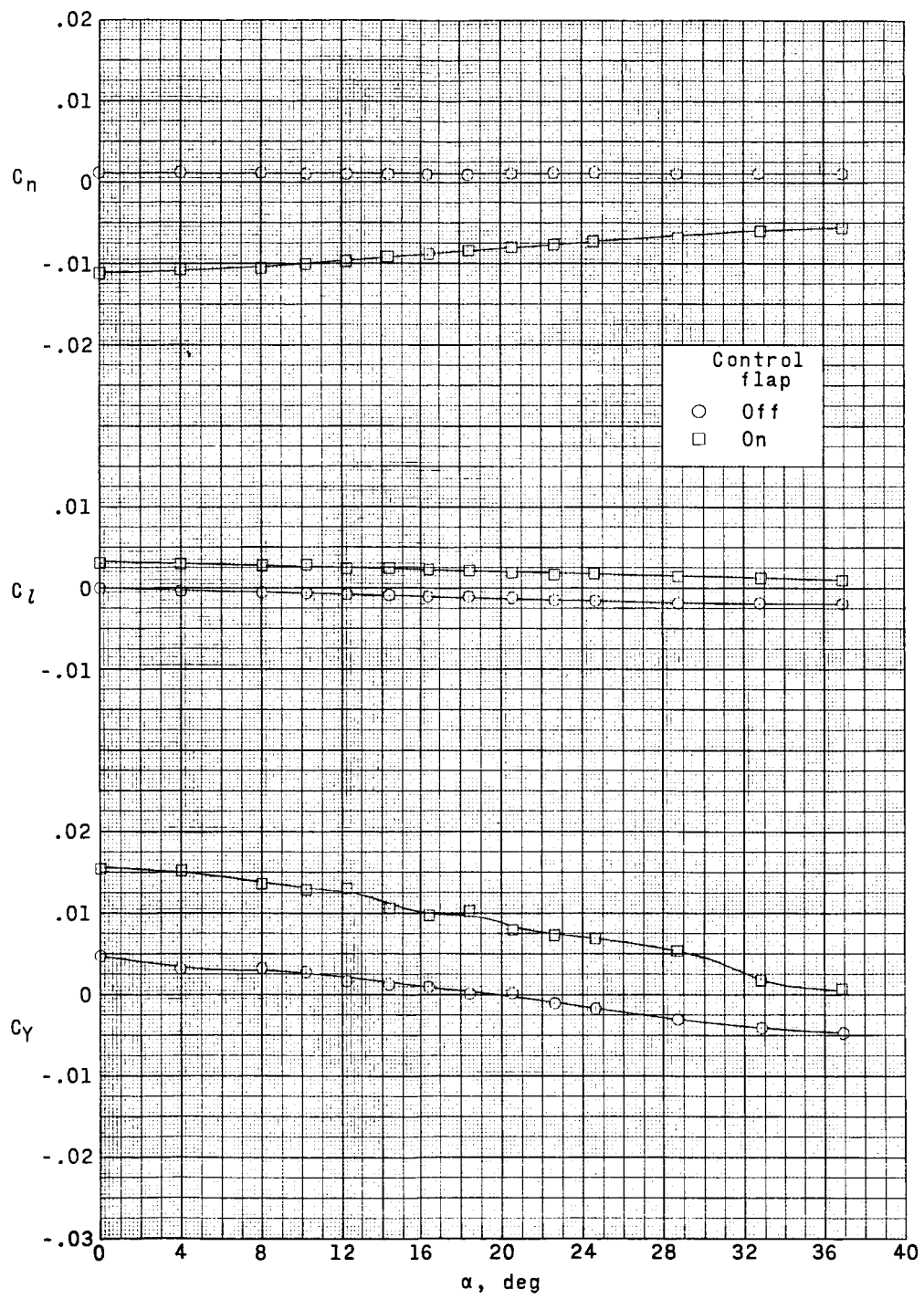
(b) $M = 1.80$.

Figure 13.- Continued.



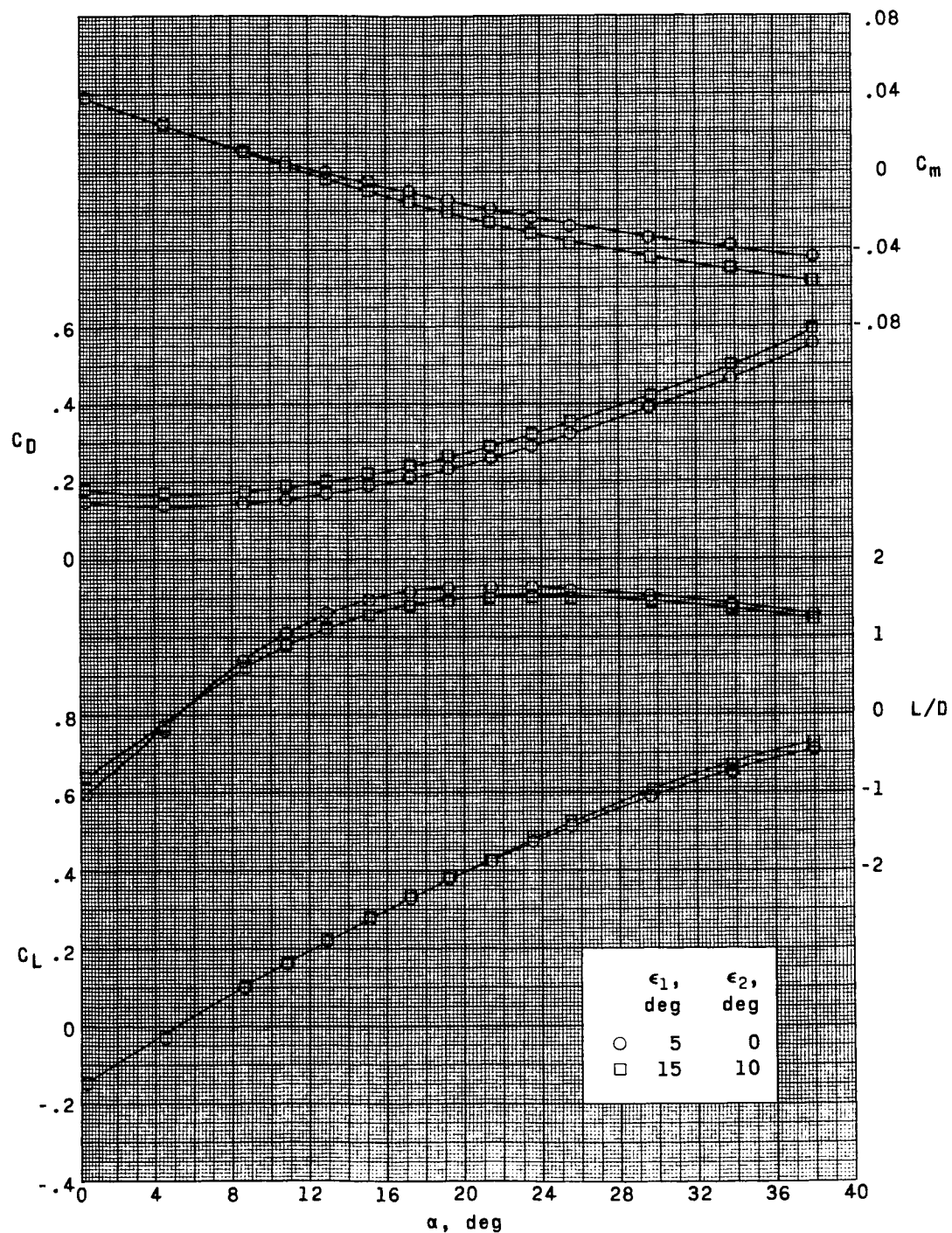
(c) $M = 2.16$.

Figure 13.- Continued.



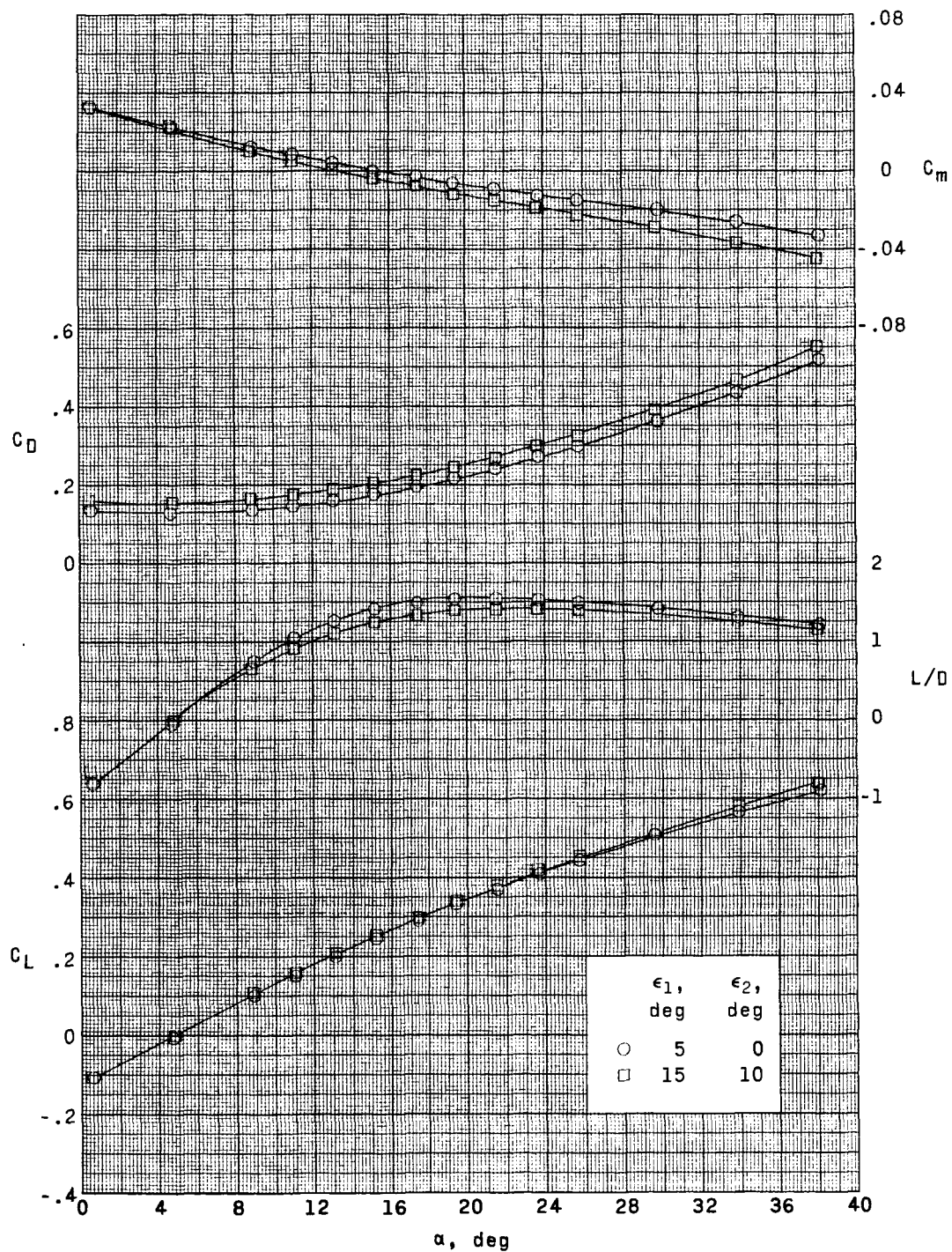
(d) $M = 2.86$.

Figure 13.- Concluded.



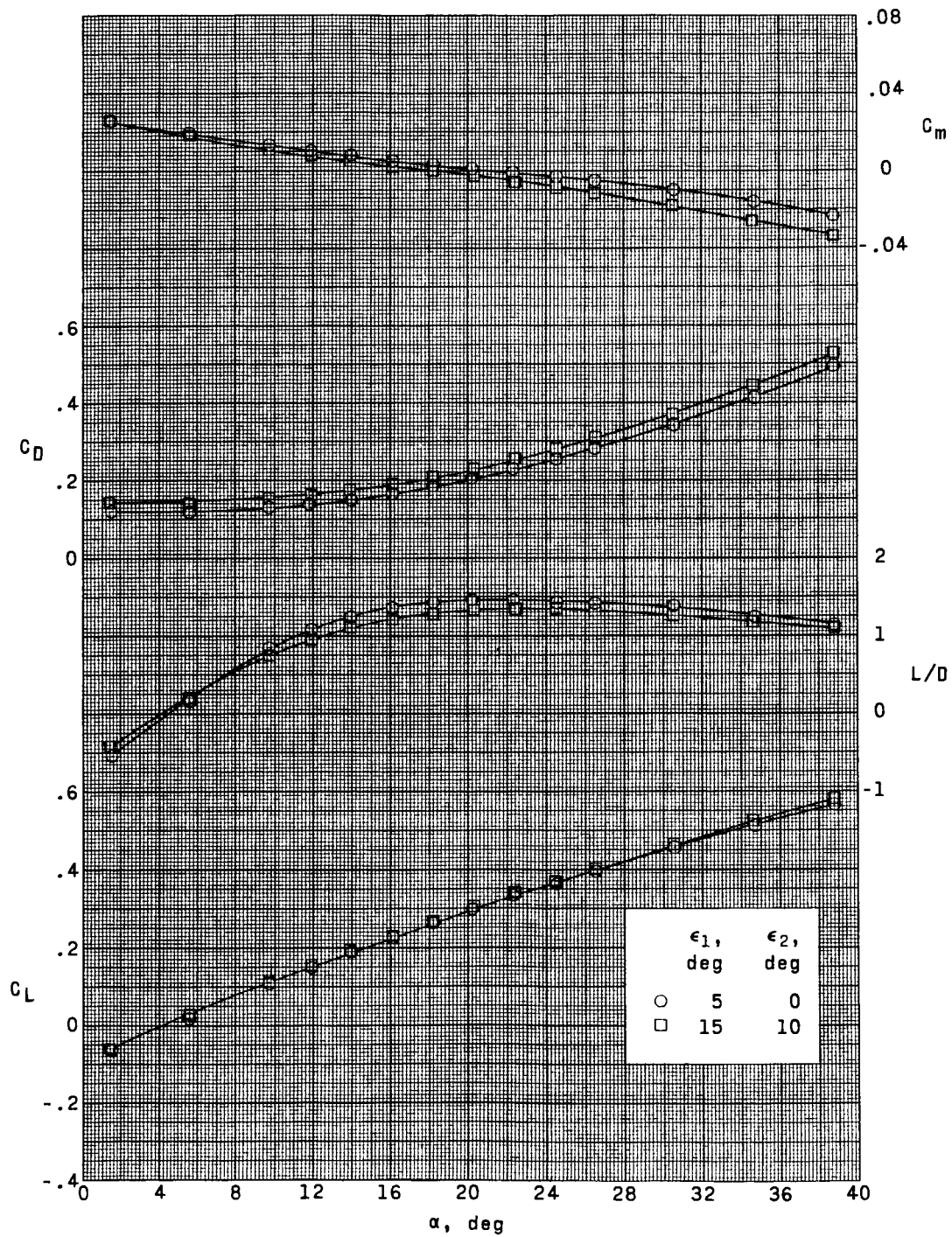
(a) $M = 1.50$.

Figure 14.- Effect of P_1 tip-fin toe-in angle on the variation of the longitudinal characteristics with angle of attack.



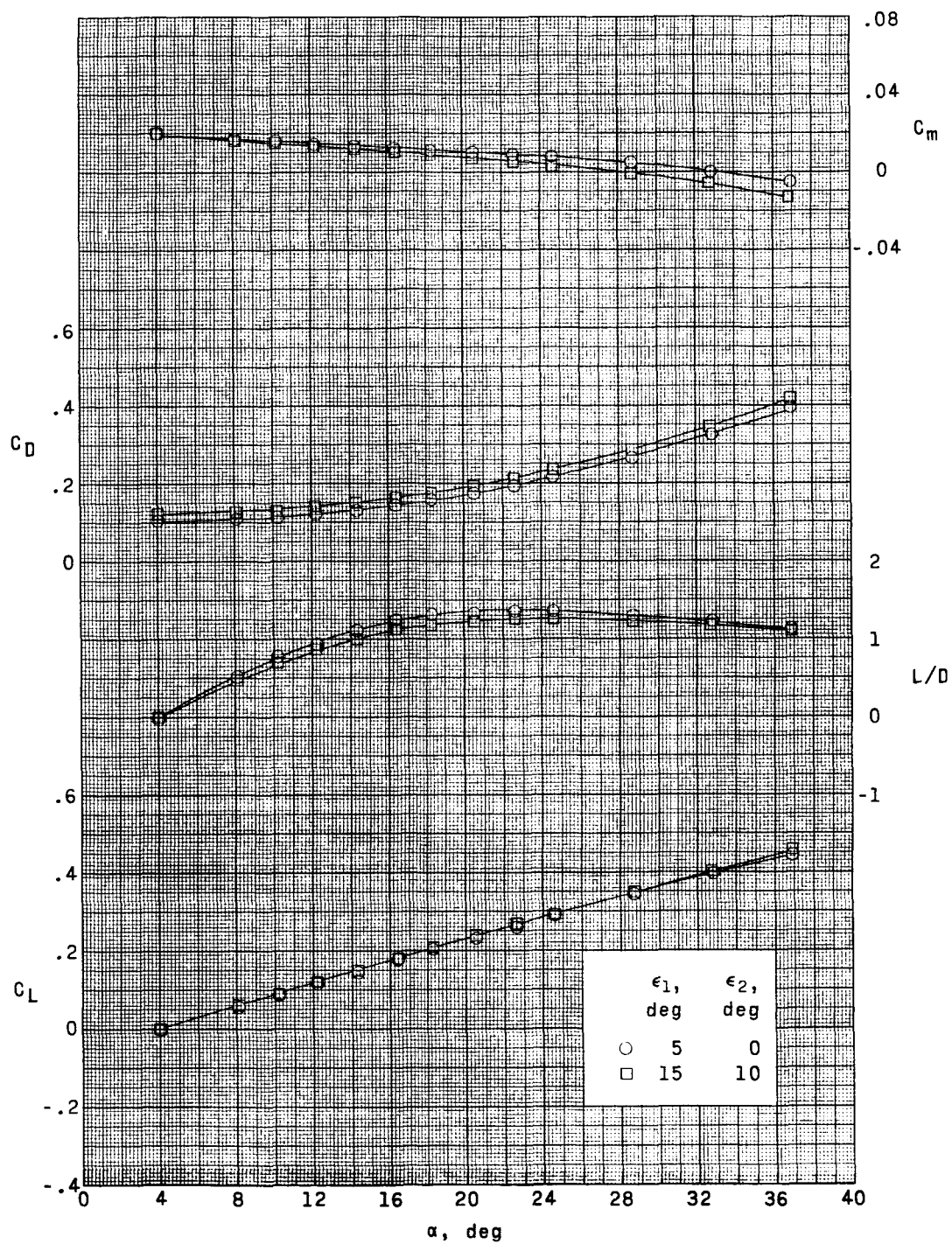
(b) $M = 1.80$.

Figure 14.- Continued.



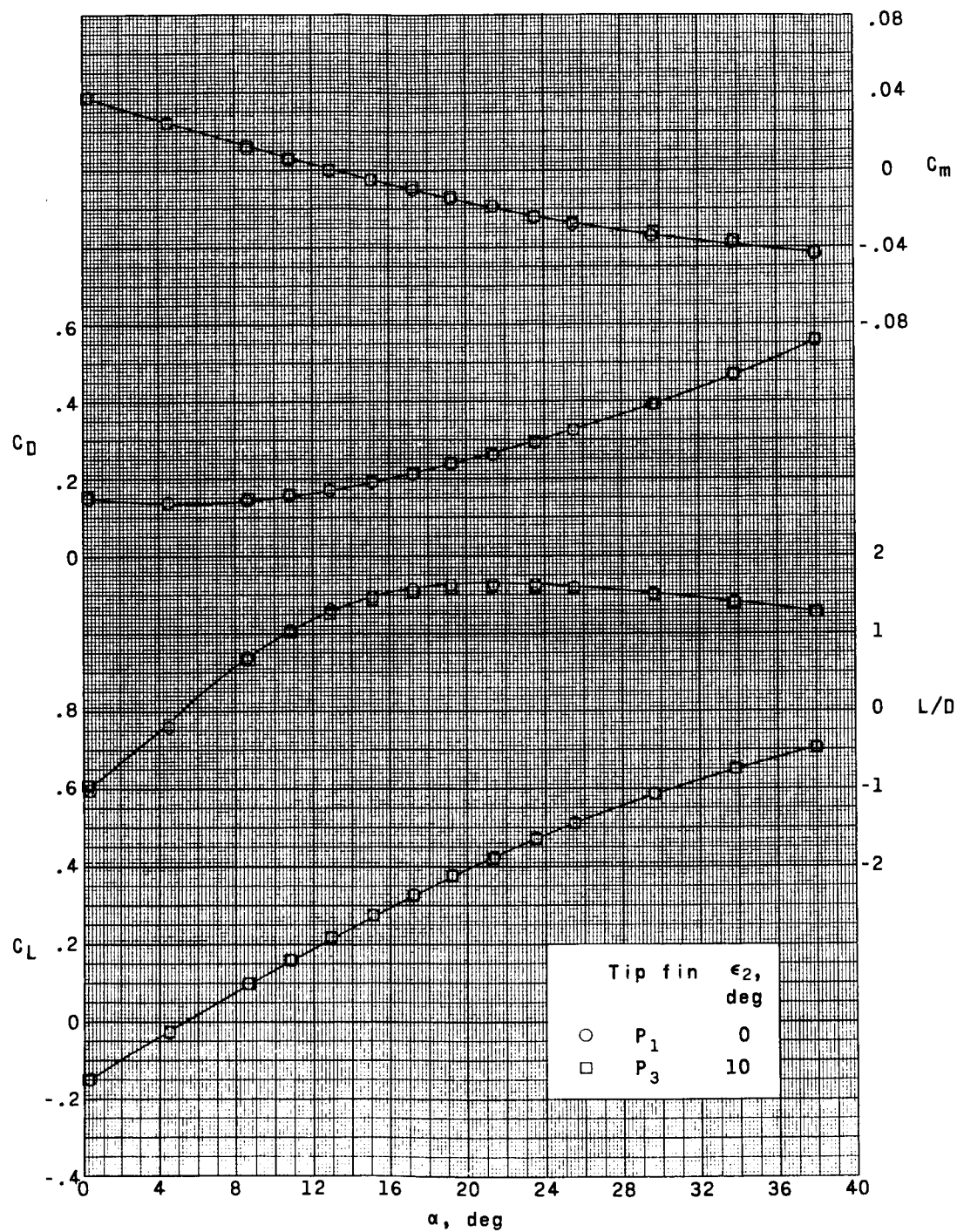
(c) $M = 2.16$.

Figure 14.- Continued.



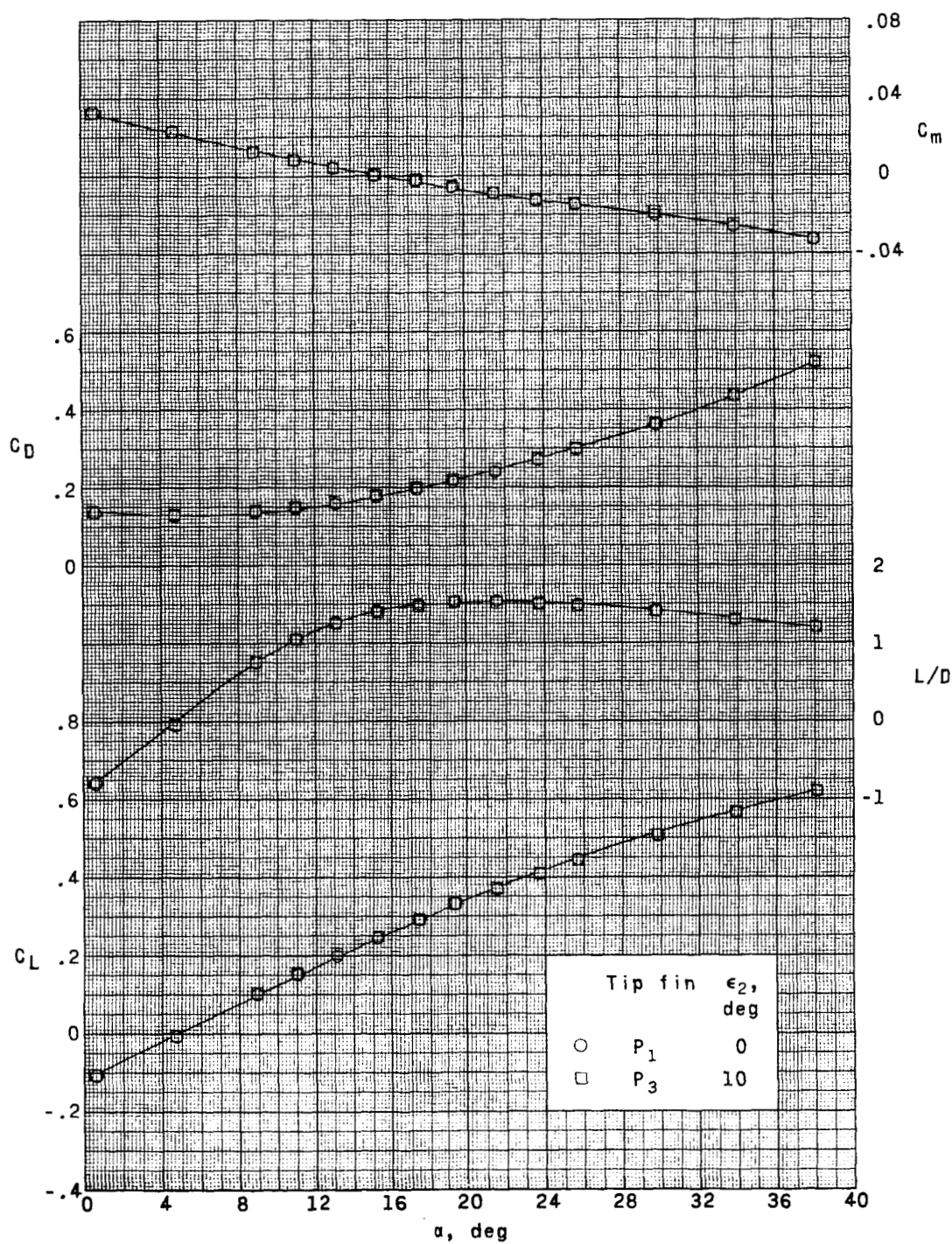
(d) $M = 2.86$.

Figure 14.- Concluded.



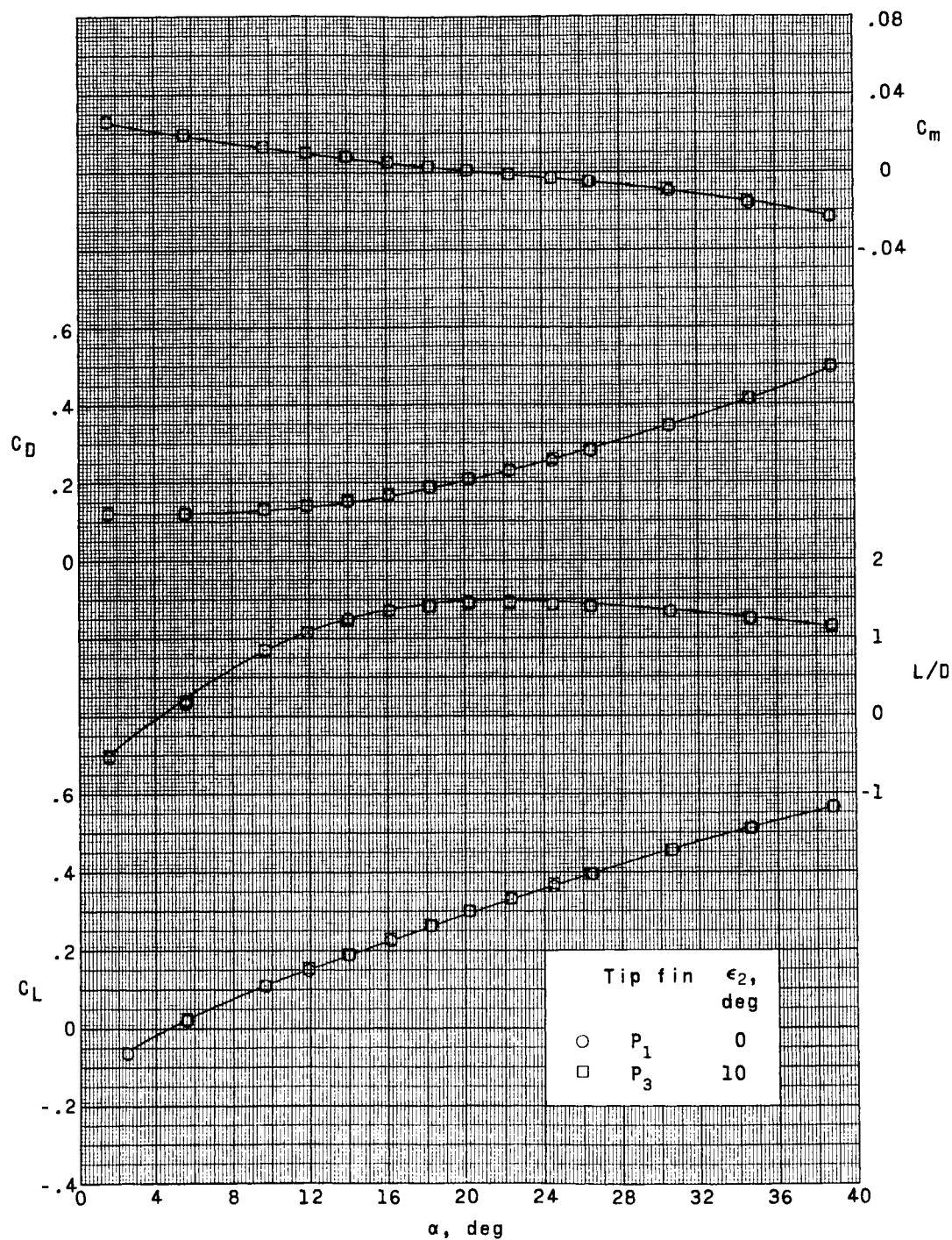
(a) $M = 1.50$.

Figure 15.- Effect of upper-panel toe-in angle (ϵ_2) on the variation of the longitudinal characteristics with angle of attack.



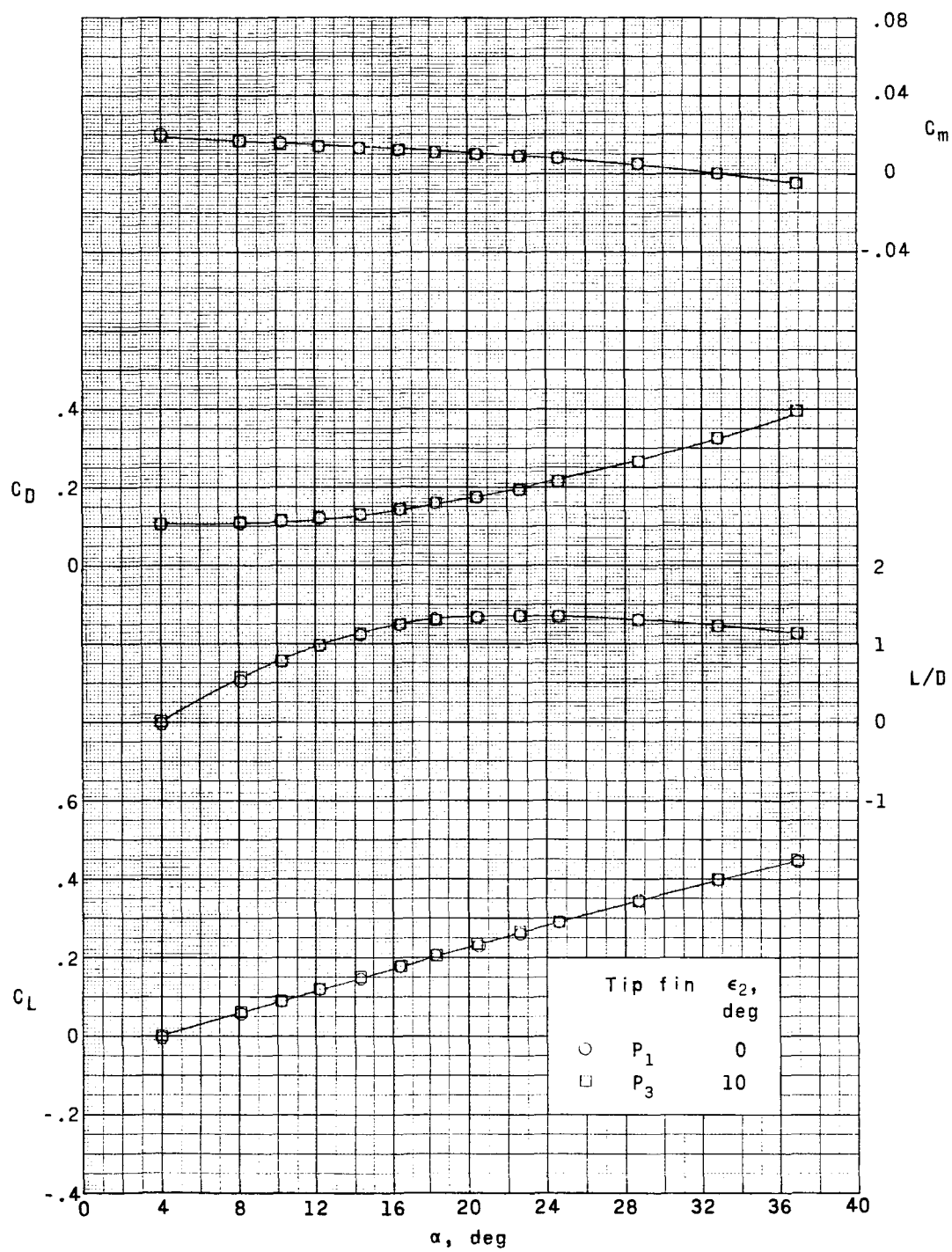
(b) $M = 1.80$.

Figure 15.- Continued.



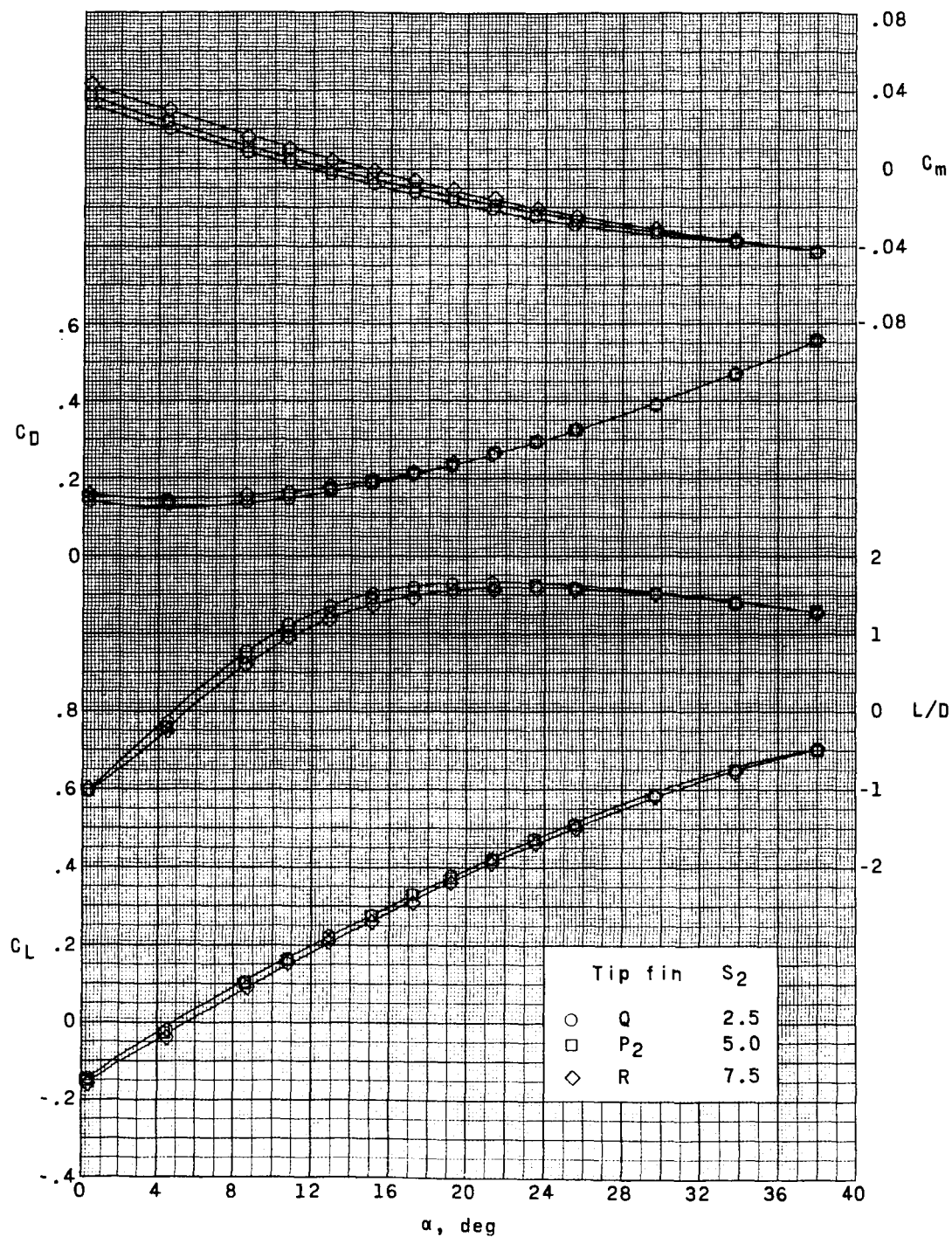
(c) $M = 2.16$.

Figure 15.- Continued.



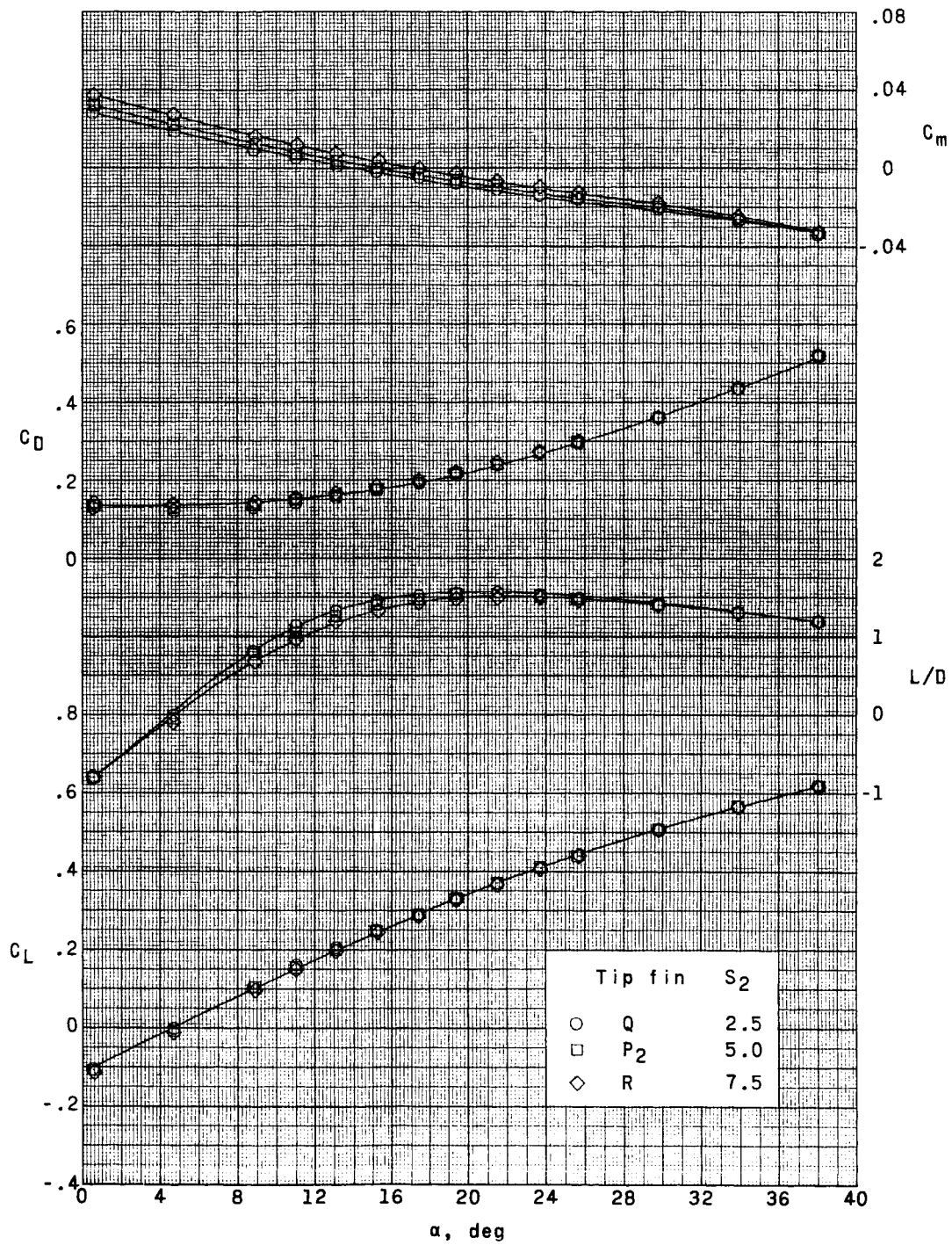
(d) $M = 2.86$.

Figure 15.- Concluded.



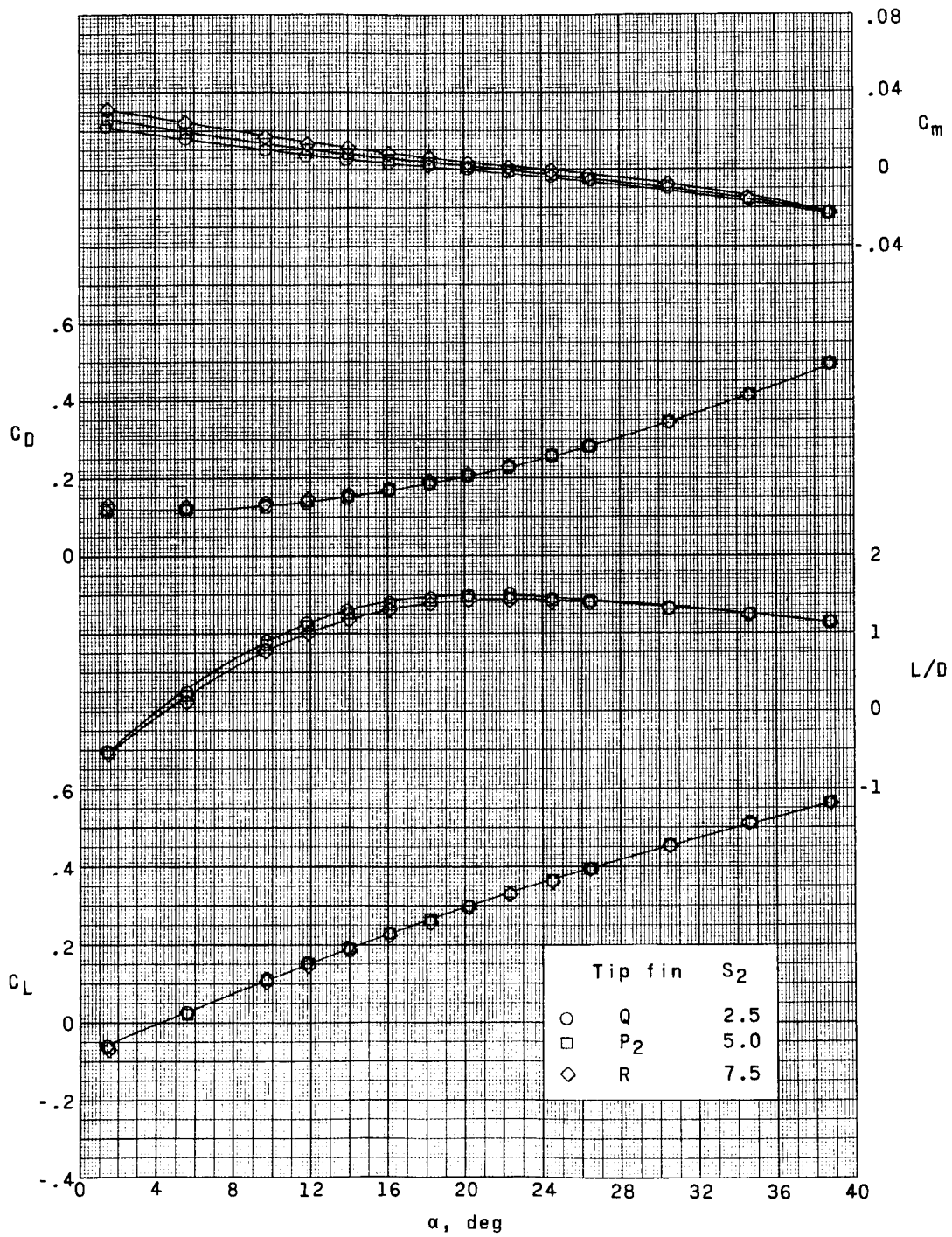
(a) $M = 1.50$.

Figure 16.- Effect of upper-panel planform area (S_2) on the variation of the longitudinal characteristics with angle of attack.



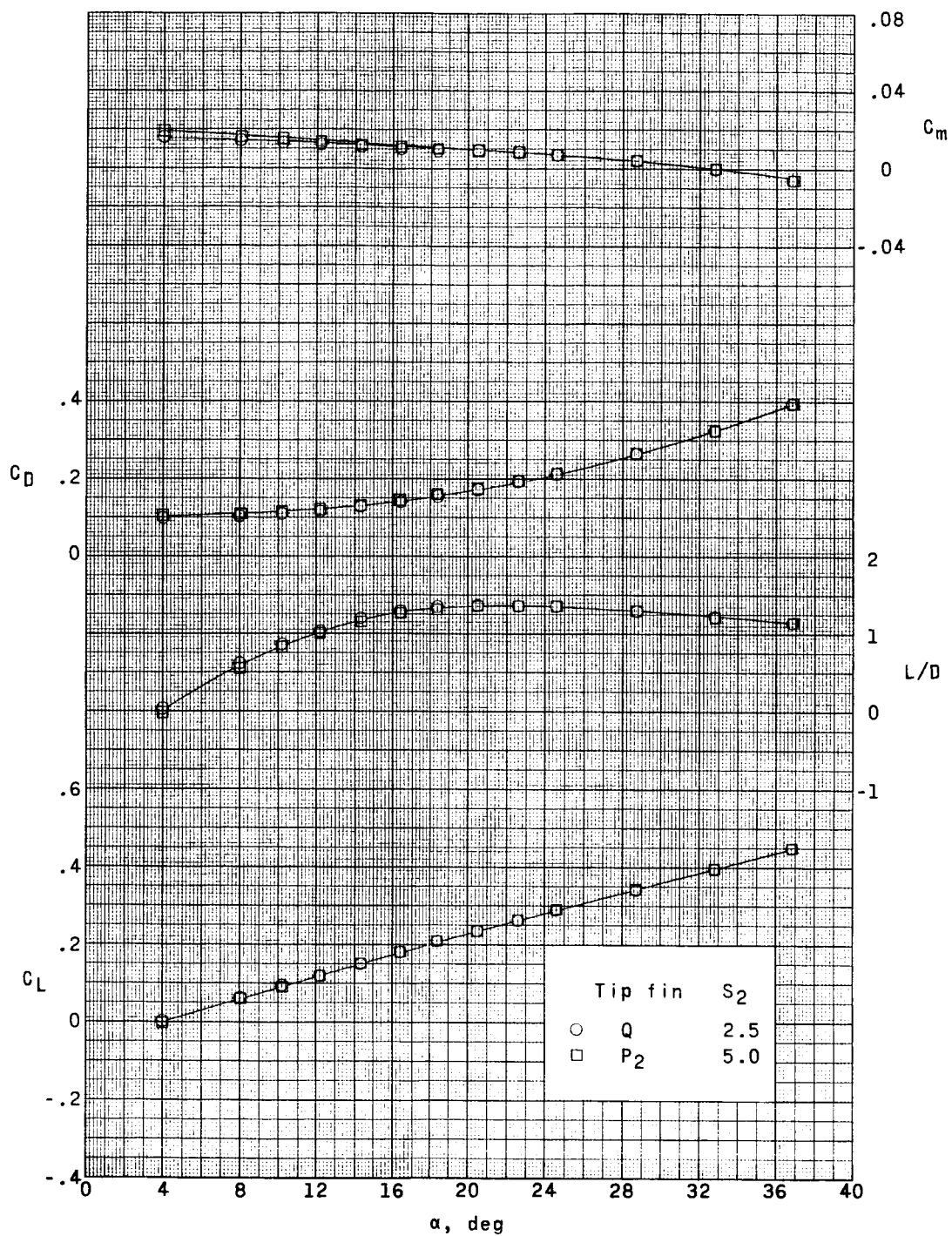
(b) $M = 1.80$.

Figure 16.- Continued.



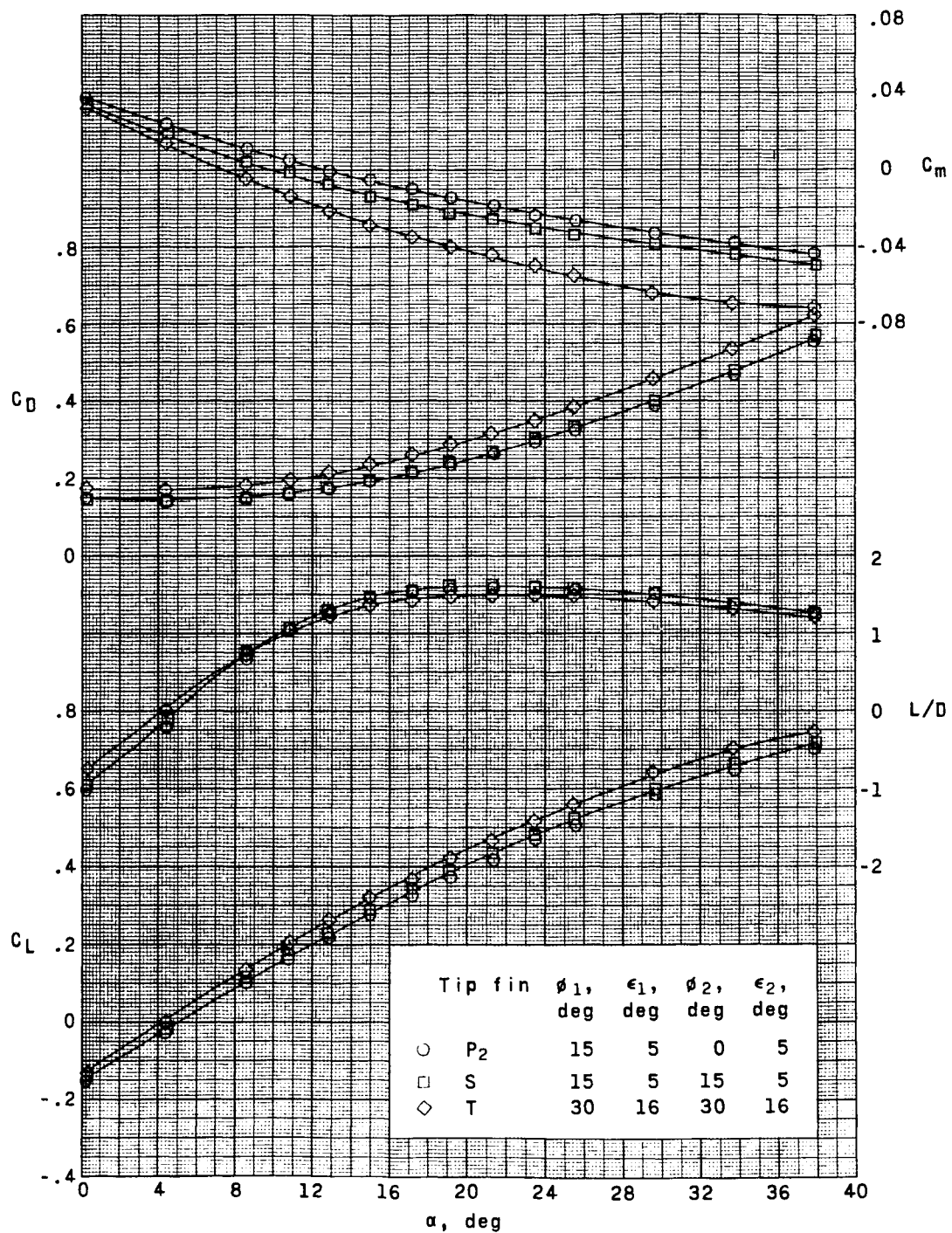
(c) $M = 2.16$.

Figure 16.- Continued.



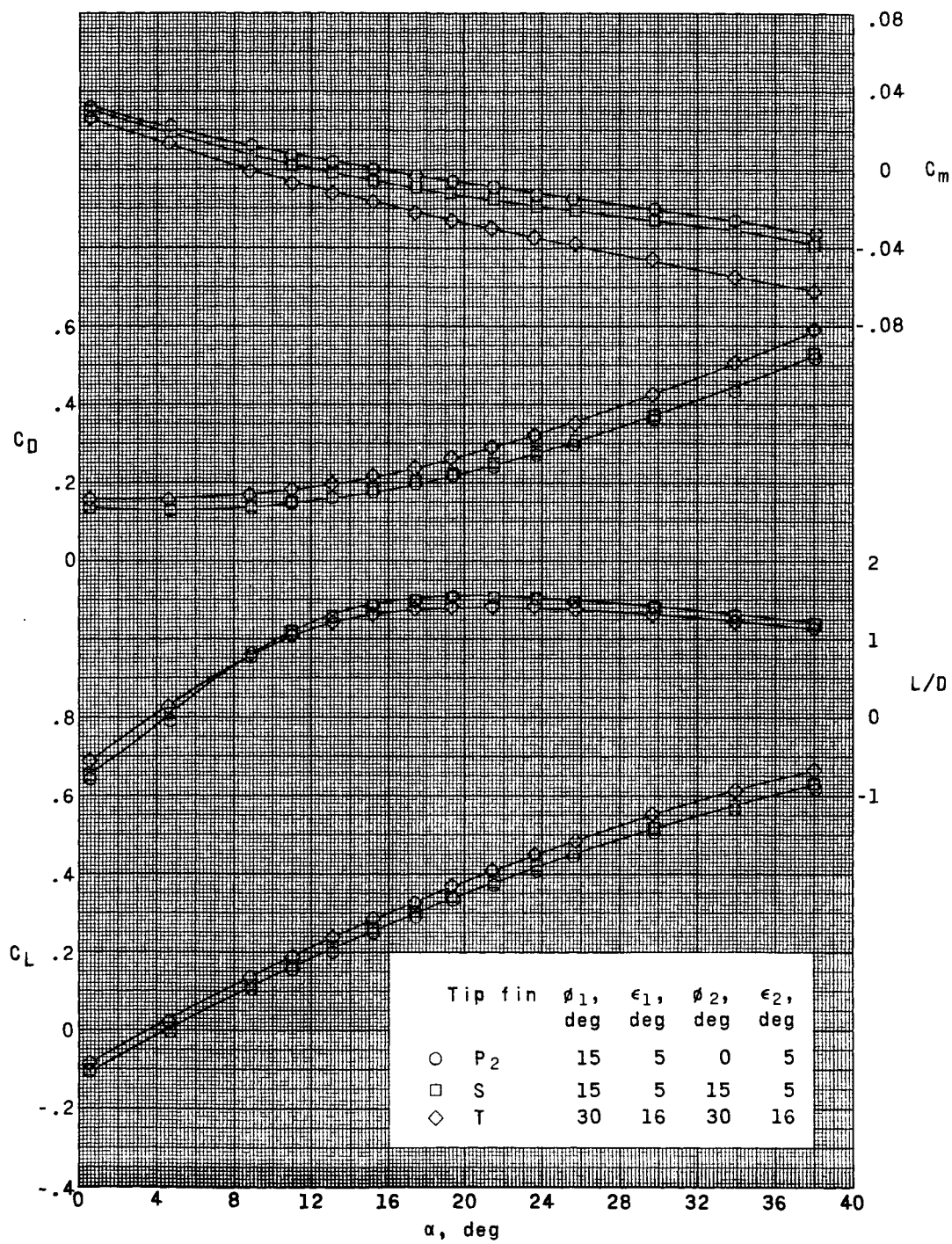
(d) $M = 2.86$.

Figure 16.- Concluded.



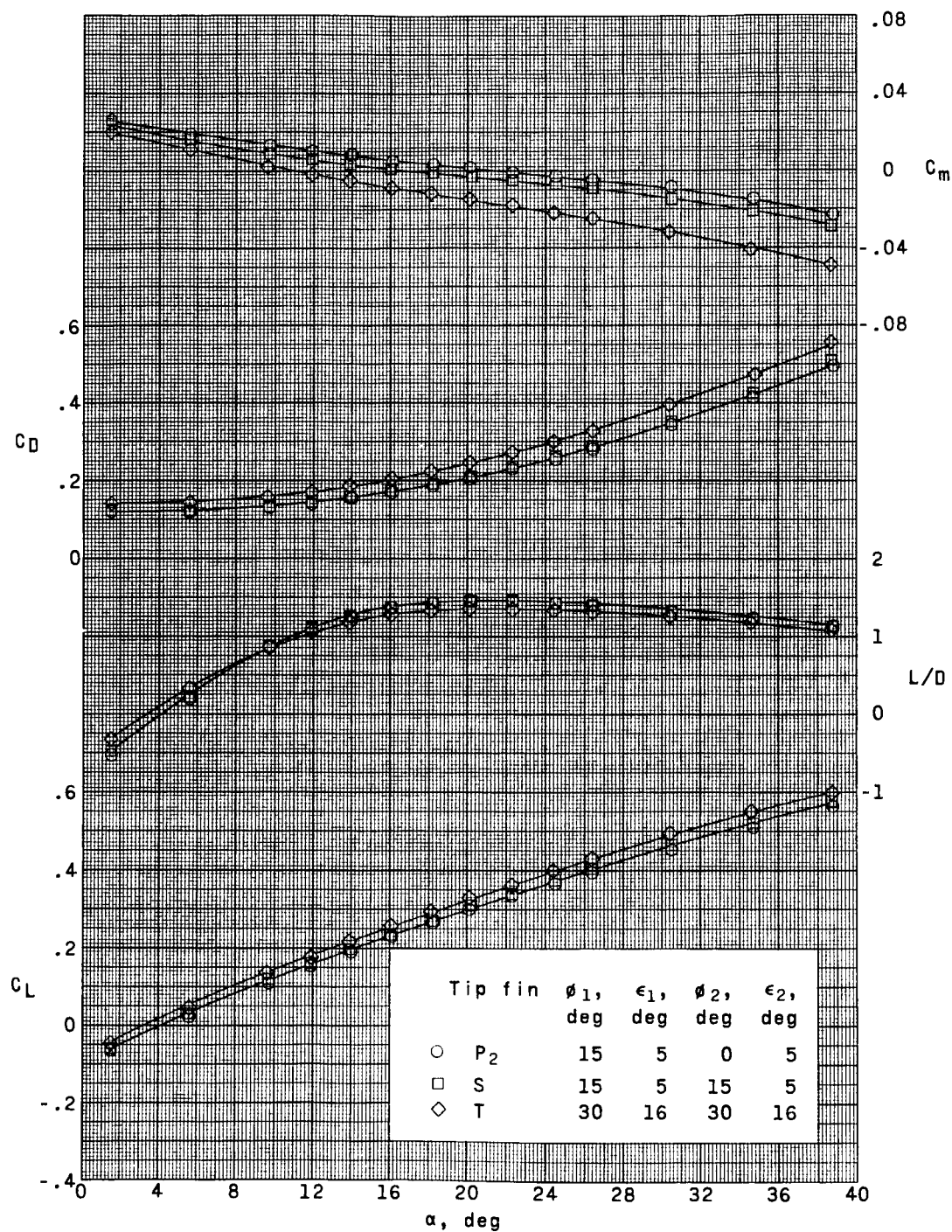
(a) $M = 1.50$.

Figure 17.- Effect of upper-panel roll-out angle (ϕ_2) on the variation of the longitudinal characteristics with angle of attack.



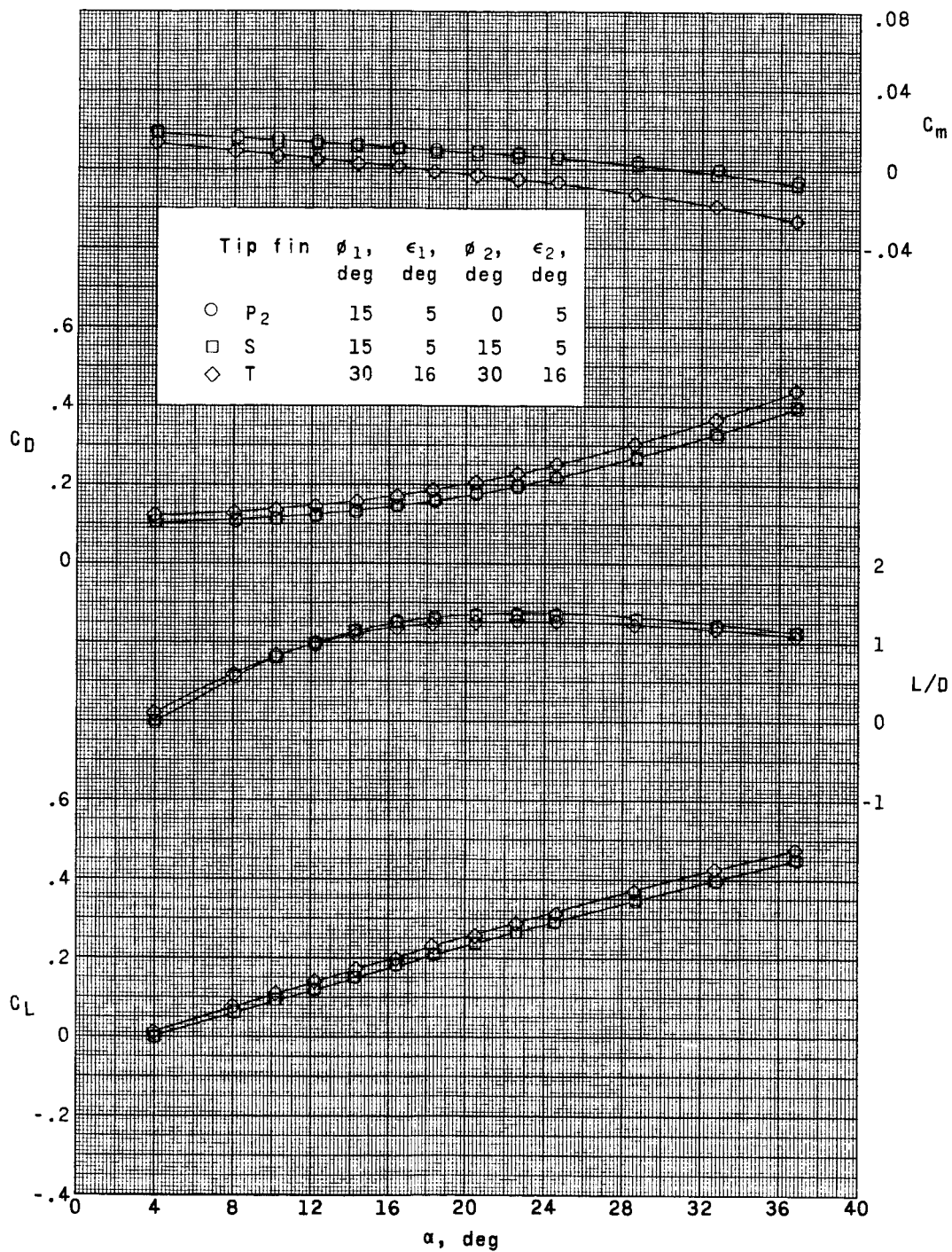
(b) $M = 1.80$.

Figure 17.- Continued.



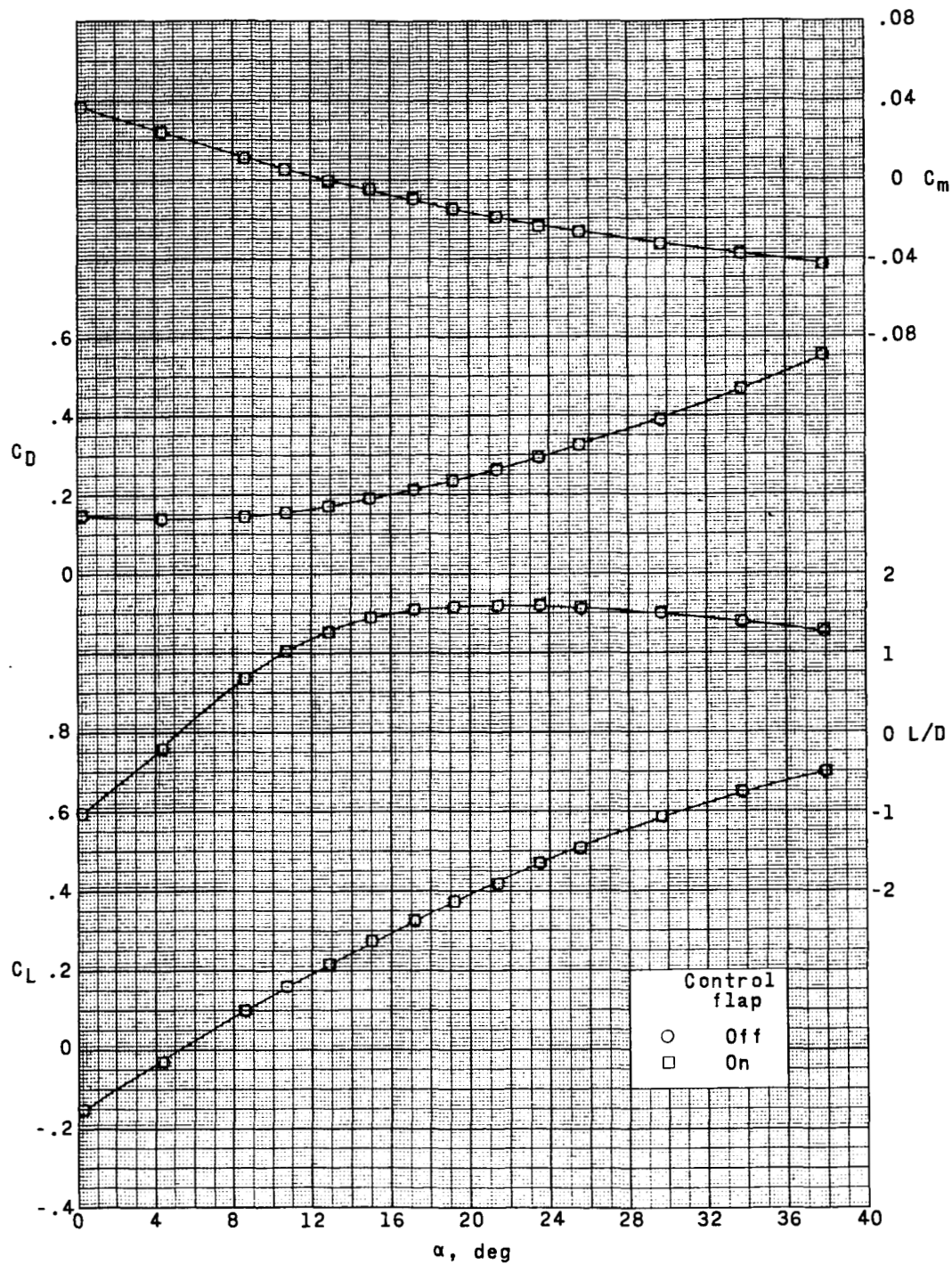
(c) $M = 2.16$.

Figure 17.- Continued.



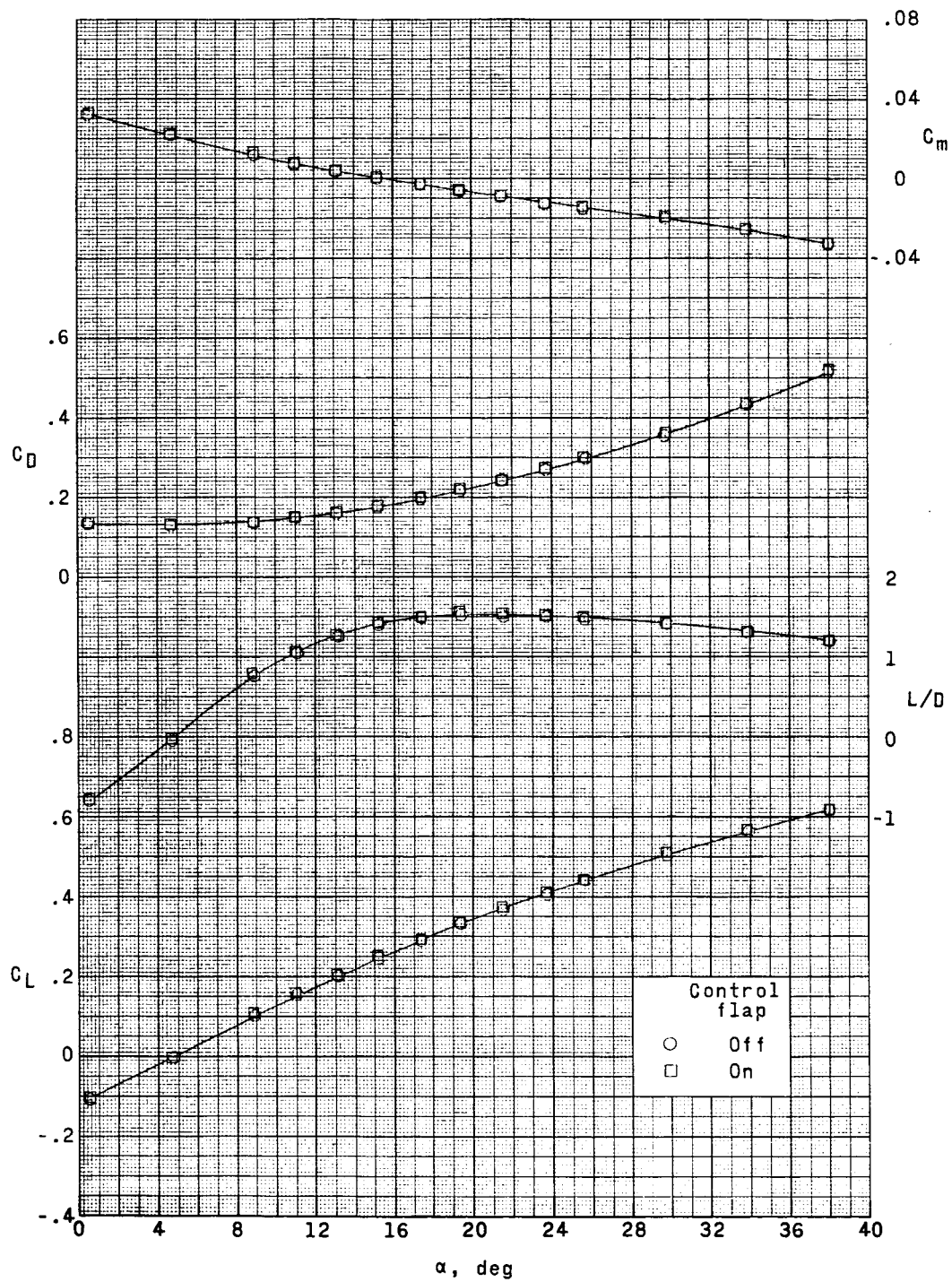
(d) $M = 2.86$.

Figure 17.- Concluded.



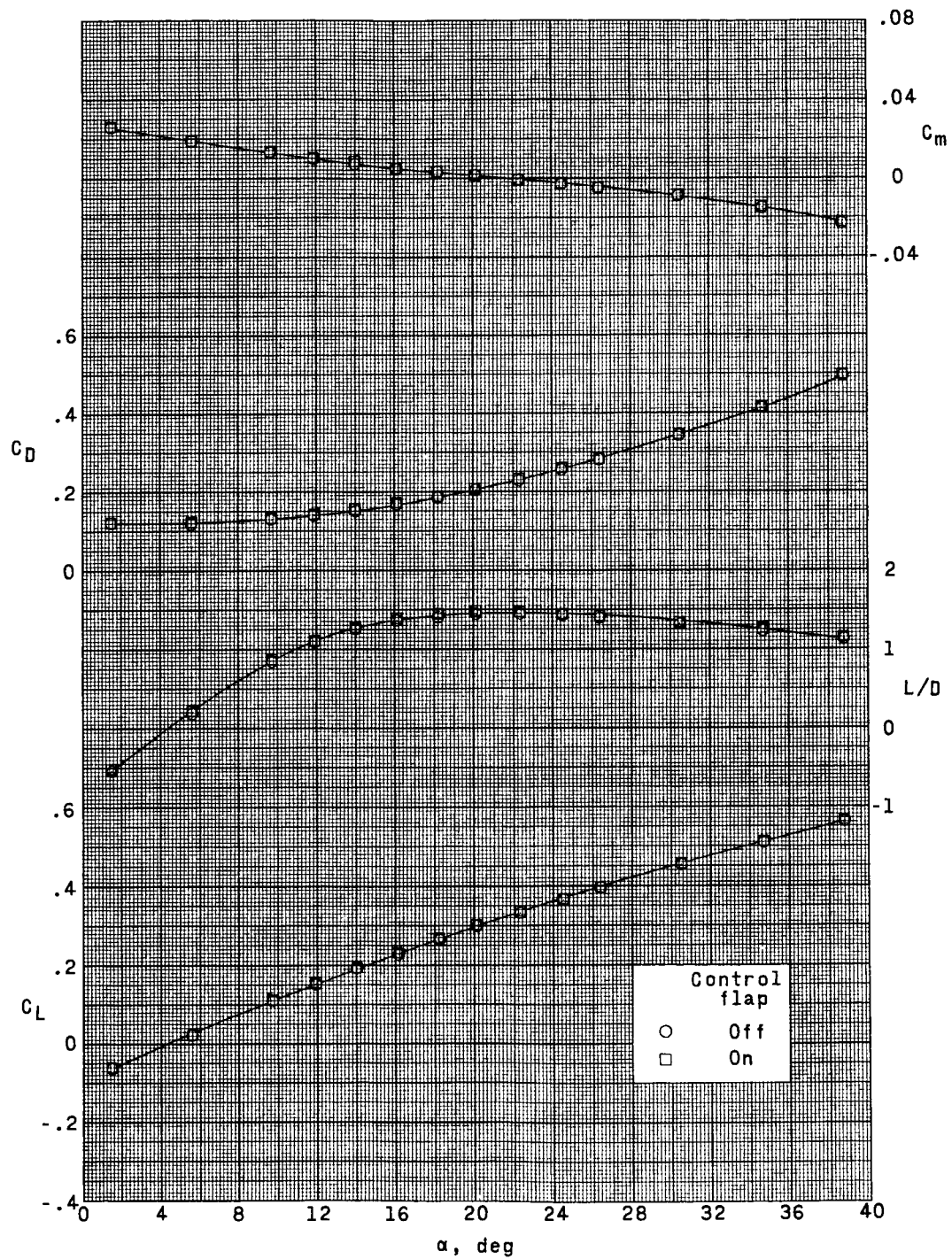
(a) $M = 1.50$.

Figure 18.- Effect of P_2 left tip-fin upper-panel control-surface deflection on the variation of longitudinal characteristics with angle of attack.



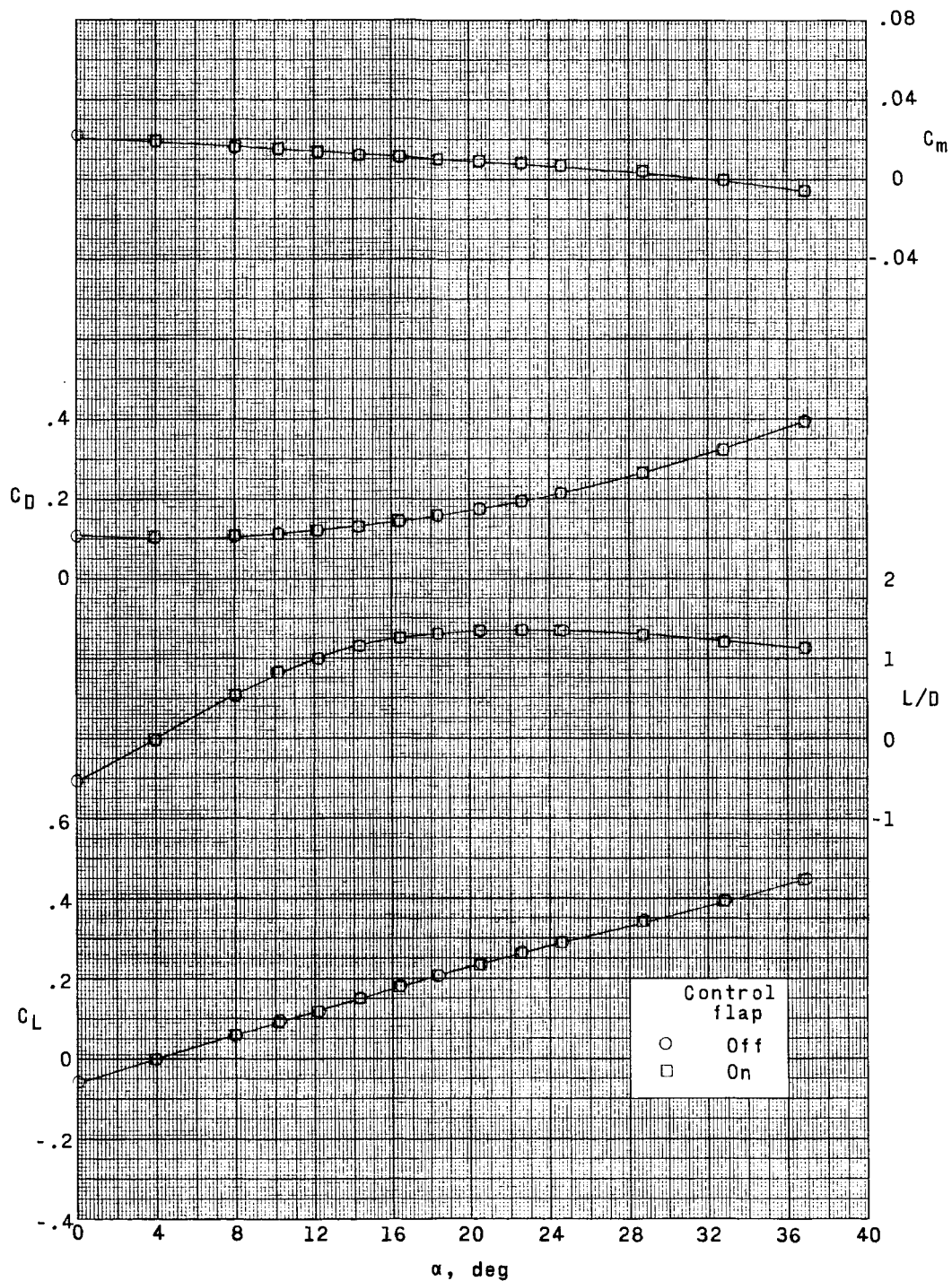
(b) $M = 1.80$.

Figure 18.- Continued.



(c) $M = 2.16$.

Figure 18.- Continued.



(d) $M = 2.86$.

Figure 18.- Concluded.